Environmental Science Advances

ROYAL SOCIETY OF CHEMISTRY

PAPER

View Article Online
View Journal | View Issue

Cite this: *Environ. Sci.: Adv.*, 2025, **4**, 1810

Critical analysis, characterization, and treatment of microplastics in the peripheral rivers of Dhaka city: Buriganga and Turag

Foysal Mahmud, [a] Hridoy Roy, *[a] Md. Mahmud Kamal Bhuiyan[a] and Md. Shahinoor Islam *[ab]

Microplastic pollution is an emerging global concern due to its persistent nature, toxic effects, and complex detection techniques. This study analyzed microplastic (MP) abundance in water and sediments of Buriganga and Turag Rivers in Dhaka city, revealing severe contamination in Buriganga (dry season: 26.98–374.84 MPs per L water, 11 360–134,330 MPs per kg sediment; wet season: 5.17–9.07 MPs per L, 2060–10,225 MPs per kg). Turag exhibited lower pollution (dry: 3.02–24.76 MPs per L, 1430–6720 MPs per kg; wet: 1.93–14.57 MPs per L, 1255–6590 MPs per kg). Dominant MPs comprised fragments/films/fibers, with sizes <300 μm (33–75% prevalence) and white particles (26–35%), supplemented by red/black (Buriganga) and brown/black (Turag). Polymers were dominated by polyethylene (75–83% occurrence) and polypropylene (83%), with polystyrene in 4–8% of samples. Moreover, the presence of toxic heavy metals, *e.g.*, Cr, Mn, Pd, Cd, Pb, was observed on the surface of MP samples. Hierarchical Cluster Analysis revealed distinct groupings of sampling stations based on the concentration and weight of MPs, highlighting spatial variations in MP distribution across rivers and seasons, while the Pollution Load Index confirmed moderate risk across both rivers, peaking at 4.11 (water) and 4.02 (sediment) in the dry season of Buriganga. Electrocoagulation (Al–Al electrodes, 15 V) achieved >99% MP removal within 150 minutes, following second-order kinetics with voltage-dependent efficiency. These findings underscore MPs as complex hazards to the environment, urging prioritized source control, scaling of remediation techniques, and standardized monitoring for urban river systems.

Received 1st May 2025
Accepted 21st August 2025

DOI: 10.1039/d5va00118h

rsc.li/esadvances

Environmental significance

Microplastic pollution represents a critical environmental challenge due to its persistence, ecosystem interactions, and potential human health impacts. This study advances the understanding of microplastic pollution in urban river systems of Dhaka city, Bangladesh, through a comprehensive assessment of microplastic contamination patterns across rivers, seasons, polymer characteristics, and presence of heavy metals. We demonstrate the efficacy of an electrochemical treatment process for mitigating microplastic pollution while discussing the fundamental removal mechanisms in a laboratory setup. The integrated approach, combining field-based microplastic pollution characterization with engineered solutions, provides actionable frameworks for developing evidence-based regulations, optimizing waste management strategies, and implementing scalable remediation technologies in rapidly urbanizing regions facing similar environmental challenges.

1 Introduction

Global plastic use has grown significantly in recent decades, and worldwide plastic production was 460 million tons in 2019, which is estimated to reach 1200 million tons by 2060.[1] Different types of polymers, such as polyethylene (PE), polypropylene (PP), polystyrene (PS), polyester (PES), polyvinyl chloride (PVC), polycarbonate (PC), and polyethylene terephthalate (PET), are widely used in a range of applications.[2–6] These polymers are extensively used commercially, industrially, and in households. PE and PS are widely used as packaging materials, while PET, PC, and high-density polyethylene (HDPE) are used for manufacturing plastic bottles.[7] However, due to rapid industrialization and improper plastic waste management worldwide, the amount of plastic waste in the environment is increasing, with approximately 400 million tons generated each year.[8] Moreover, the plastic recycling rate is very insignificant. In 2019, only 9% of plastic waste was recycled.[1] Worldwide, 85% of packaging products ultimately find their way into landfills and contribute to plastic pollution.[8] Bangladesh, being a developing country, generates

[a]*Department of Chemical Engineering, Bangladesh University of Engineering and Technology, Dhaka-1000, Bangladesh. E-mail: hridoyroy@che.buet.ac.bd; shahinoorislam@che.buet.ac.bd*

[b]*Department of Textile Engineering, Daffodil International University, Dhaka 1341, Bangladesh*

almost 1.095 million tonnes of plastic waste every year.[9] Every day, approximately 646 tons of plastic waste are collected by Dhaka North City Corporation (DNCC) and Dhaka South City Corporation (DSCC) combined. Unfortunately, only 37% of the plastic waste in DNCC and DSCC is efficiently recycled, and a majority of the plastic waste makes its way into adjacent canals and rivers.[10] Since plastic is non-biodegradable, a huge amount of waste plastics is sustained in the environment for a long period of time, and contributes to the secondary microplastics (MPs) in the environment.[11] Although secondary MPs result from the long-term breakdown of large plastic waste, they are currently considered the main contributor to environmental MP pollution.[12]

In recent times, MP pollution has gained significant attention due to its non-biodegradability and potential impact on ecosystems, wildlife, and human health.[13] Extensive studies have been conducted to evaluate the toxicity of MPs. Zhang *et al.* (2017) showed that MP PVC particles with a diameter of 1 μm significantly inhibited algal growth, resulting in a maximum growth inhibition ratio of 39.7% after 96 hours of exposure.[14] Choi *et al.* (2018) reported that both spherical and irregularly shaped MPs accumulated in the digestive system of the sheepshead minnow, resulting in intestinal distention. Moreover, the irregular microplastics significantly reduced swimming behavior.[15] To avoid MP contamination, aquatic organisms may modify their feeding behavior, while the continued accumulation of microplastics may contribute to the decline of fish stocks and pose risks to ecosystem stability.[16,17] MPs pose significant risks not only to aquatic life but also to human health. Although direct studies on the effects of MPs on human health are limited, recent research using model organisms and cell cultures suggests that MPs may induce immune responses, oxidative stress, and reproductive or developmental toxicity.[18] Similarly, Li *et al.* (2023) reported that toxicological studies employing cells, organoids, and animal models have shown that microplastics can cause a variety of adverse effects, including oxidative stress, DNA damage, organ dysfunction, metabolic disturbances, immune responses, neurotoxicity, and reproductive and developmental toxicity.[19] Therefore, studying the presence of MPs in the environment is crucial, as understanding their abundance assists evaluation of the intensity of pollution and identifies regions with high levels of contamination.[20] Moreover, the MP abundance study will facilitate the determination of the sources and pathways of MPs. The obtained data will be useful for developing guidelines and regulations to reduce MP pollution, implementing effective waste management strategies, encouraging sustainable practices, and reducing the MP release at their origin.[21–23]

MP pollution typically comes from terrestrial sources and is distributed mostly by hydrological and atmospheric media before accumulating in terrestrial, freshwater, and marine environments. According to UNEP, approximately 1000 rivers are responsible for almost 80% of the plastic that enters the ocean each year, ranging from 0.8 to 2.7 million tonnes.[8] That's why rivers hold immense importance as substantial contributors to MP pollution.[24] As a riverine country with an expanding plastics market and limited waste management infrastructure, the rivers of Bangladesh face a significant threat from microplastic pollution.[9] The Buriganga and the Turag rivers, which flow around the capital city of Bangladesh, are among the most heavily polluted rivers in the country due to the intense discharge of industrial and municipal waste.[25–29] These two rivers are very important due to their critical pollution status and regional importance in Dhaka. As primary drainage channels, they receive a significant amount of plastic waste daily[10] and exhibit severe heavy metal levels in sediments that exceed safety limits,[26] threatening ecosystems serving over 4 million residents. Critically, seasonal variation, particularly the dry–wet cycle governing these river systems, remains unquantified for MP pollution in these rivers despite its known impact on hydrological transport mechanisms. Hence, the current study focuses on the assessment of the identification and quantification of MPs in the Buriganga and the Turag rivers in two different seasons. Furthermore, conventional water treatment plants cannot remove MPs completely.[30–32] More than 4 million MPs per day are reported to be released from each wastewater treatment plant (WWTP).[33] Most of the particles found in the treated water from a WWTP are less than 10 μm.[30] However, conventional WWTPs cannot successfully remove MPs smaller than 100 μm.[34] Several treatment processes are being studied for the treatment of MPs, such as bacterial degradation, thermal degradation, electrocoagulation, advanced oxidation processes, and adsorption.[35–37] Electrocoagulation (EC) is an efficient technique for water treatment that has the potential to remove such small MP particles.[33,38–42] The fundamental idea behind the EC process is electrolysis, where the generated metal cations from the anode participate in the production of micro-coagulants. These coagulants destabilize the suspended particles, *e.g.*, MPs in the water, by binding them and settling as flocs.[43] Most of the recent literature reported an efficiency between 90 and 99.5% in the treatment of different types of MPs from water. Most of these studies used simulated water samples or wastewater from wastewater treatment plants.[33,44–47] Notably, there are limited studies on EC treatment of MPs using actual river water samples, creating a methodological gap especially relevant for complex urban rivers like the Buriganga and Turag.

This study therefore addresses two key research needs in the Buriganga and Turag rivers, *e.g.*, (1) comprehensive seasonal assessment of MP pollution across water and sediment matrices, including characterization of physical properties (morphology/size/color), polymer composition, and heavy metal adsorption; and (2) evaluation of EC treatment efficacy for natural river water, targeting high MP removal under operational voltages with kinetic analysis to understand in-depth removal mechanisms.

2 Materials and methods

2.1. Study area

The study was conducted along the Buriganga and Turag rivers in Dhaka, Bangladesh, which receive substantial wastewater inputs from the metropolitan area. Twelve sampling stations (six per river) were established following a systematic naming

convention where each sample was coded by the river (B for Buriganga, T for Turag), matrix (W for water, S for sediment), season (D for dry season from January to March, W for wet season from July to September), and station number (1–6). The sampling design included industrial zones (B4 near Chandir Ghat recycling facilities, T1 near textile mills), urban residential areas (B1–B3 in central Dhaka, T3–T5 in Ashulia), and upstream-downstream transects (B5–B6, T2, T6) to capture spatial variations in microplastic distribution. Coordinates and site characteristics are detailed in Table 1. The spatial distribution is presented in Fig. 1, created using ArcGIS 10.8.2 with hydrological data from the Bangladesh Water Development Board. This approach enabled consistent sample identification while examining microplastic patterns across different land uses and seasonal flow conditions characteristic of the monsoon climate of the region.

2.2. Sample collection

The surface water sample was collected from designated points, as depicted in Fig. 1, using a bucket and a plankton net with a pore size of 50 μm. The top 25 cm of the water surface was collected using a bucket or beaker, which was then poured into the plankton net to separate the solid particles. This process was repeated until 100 L of water was sampled from each sampling point. During each sampling operation, the net was cleaned with distilled water to prevent contamination. After sample collection, the sample was stored in an amber glass bottle and sealed properly with a cap. A total of 100 L of water was collected from each sampling point. The upper 2–3 centimeters of the sediments were collected using a shovel. The sample was stored in a glass beaker with aluminum foil coverings. Bulk water samples were collected from both rivers (only from T3 and B4) using a glass beaker for the removal process. All samples were kept in a freezer in the laboratory at 4 °C for a brief period before being processed. Sample processing was initiated within 12 hours of its collection. The MP size range studied in this research is summarized in Fig. S1.

2.3. Sample processing and MP isolation

2.3.1. Sample processing and MP isolation from water. Each sample was carefully filtered using a stacked arrangement of 4.75 mm (No. 4) and 45 μm (No. 325) stainless steel mesh sieves. This 4.75 mm (No. 4) sieve was employed as a substitute instead of the desired 5 mm sieve due to unavailability. The sample portion that passed through the No. 4 sieve and was retained on the No. 325 sieve was thoroughly rinsed using distilled water. The material retained on the 4.75 mm sieve was discarded. Using a spatula, the solids accumulated in the No. 325 sieve were transferred into a clean and dry beaker (500 mL). The transfer of all particles into the beaker was ensured by rinsing the sieve carefully with a minimum amount of distilled water using a wash bottle. Then, the samples were oven-dried at 80 °C until a constant weight was achieved. Then, 20 mL of aqueous 0.05 M Fe^{2+} solution was added to the beaker of collected solids, followed by 20 mL of 30% H_2O_2. This H_2O_2 is used for digesting the organic materials present in the samples. The digestion capability of H_2O_2 is increased by adding Fe^{2+}, which acts as a catalyst. This mixture of Fe^{2+} and H_2O_2 is known as a wet peroxide oxidation (WPO) solution.[48] The solution is susceptible to vigorous boiling above 75 °C. Hence, the mixture was allowed to rest at room temperature for 5 minutes. A stir bar was introduced into the beaker to facilitate mixing, and the beaker was subsequently covered with a Petri dish. The mixture was then heated to a controlled temperature of 75 °C on a magnetic hotplate. This reaction has the potential to overflow. For safety measures, the beaker was moved from the hotplate as soon as the gas bubbles were observed in the beaker. To mitigate any potential overflow caused by the reaction, the beaker was subjected to a water bath for a short period of time. Heating was continued at 75 °C for an additional 30 minutes. If any organic matter remained visible, 20 mL of 30% hydrogen peroxide was added. The procedure was conducted repeatedly until all traces of natural organic material were no longer visible. To increase the density of the aqueous solution, approximately 6 grams of NaCl per 20 mL of the sample were

Table 1 Name of the sample, sampling sites, coordinates (latitude and longitude), and dominant pollution sources of sites used in this research

No.	Sample name	Sampling sites	Coordinates		Dominant pollution sources
			Latitude	Longitude	
1	B1	Pagla Ghat, Dhaka	23°39′40.3″N	90°27′15.1″E	Urban runoff, municipal wastewater
2	B2	Postogola Bridge, Dhaka	23°41′16.0″N	90°25′37.8″E	Mixed urban/industrial discharge
3	B3	Sadarghat Launch Terminal	23°42′21.6″N	90°24′20.8″E	Launch operations, plastic waste
4	B4	Chandir Ghat	23°42′39.8″N	90°23′26.5″E	Local plastic recycling industries
5	B5	Kholamora Ghat, Kamranghirchar	23°42′53.0″N	90°21′34.9″E	Residential wastewater
6	B6	Gudaraghat, Hazaribag	23°44′02.1″N	90°21′13.9″E	Tanneries (relocated to Hemayetpur), industrial effluents
7	T1	Near Fulpukuria Thread & Accessories Ltd, Tongi, Gazipur	23°53′51.6″N	90°26′05.4″E	Textile dyeing effluent
8	T2	Near Tongi Rail Bridge, Gazipur	23°52′55.4″N	90°24′20.3″E	Transport-related runoff
9	T3	Ashulia Kacha Bazar	23°53′48.0″N	90°20′03.3″E	Market waste, urban runoff
10	T4	Ashulia Landing station	23°53′29.5″N	90°21′34.7″E	Mixed residential/commercial waste
11	T5	Rustompur Ghat, Mirpur road	23°52′29.2″N	90°21′00.8″E	Construction runoff
12	T6	Diabari Ghat, Mirpur road	23°47′53.9″N	90°20′24.2″E	Agricultural runoff mixing zone

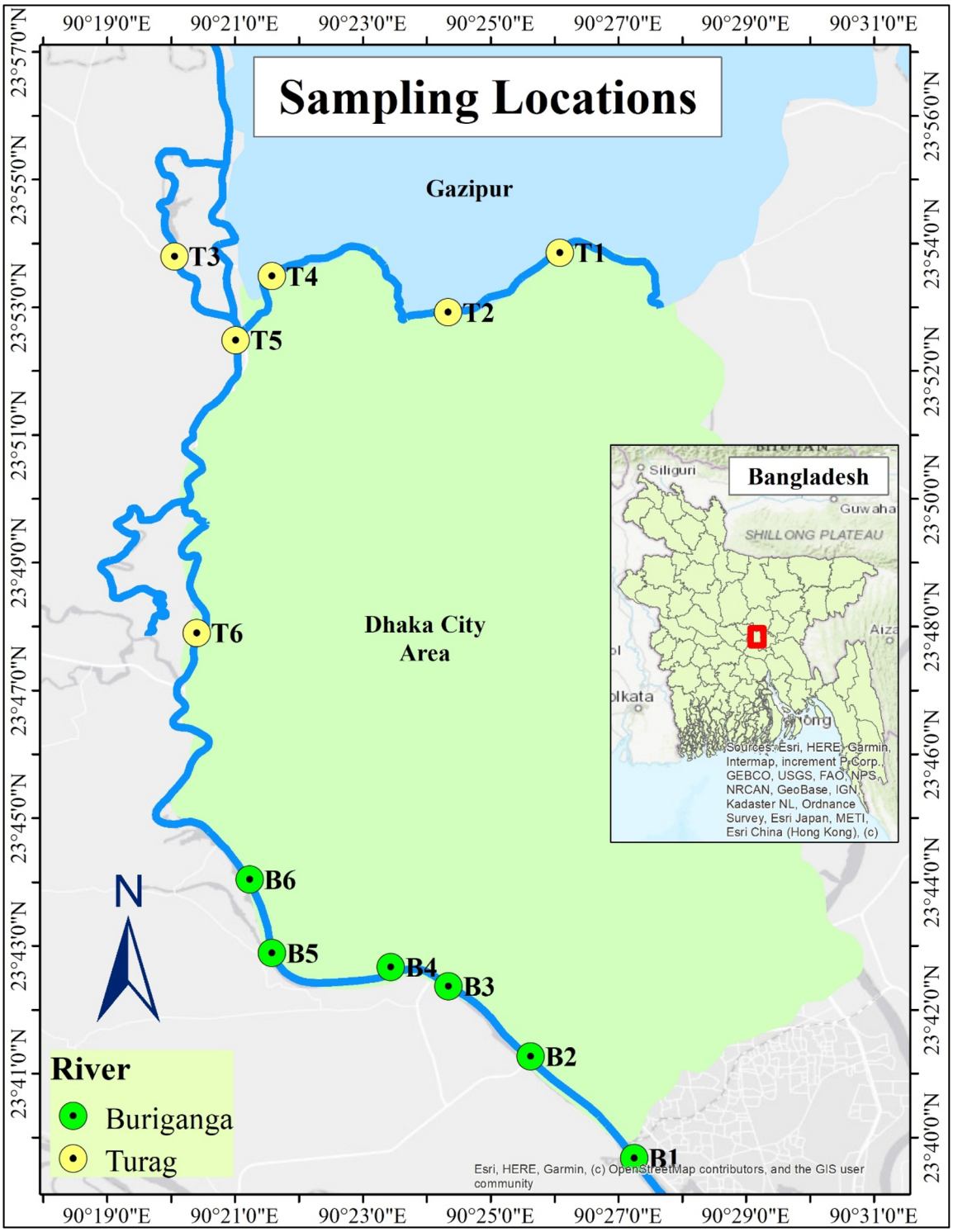

Fig. 1 Sampling points in the Buriganga and Turag rivers (map created using ArcGIS 10.8.2 software).

added, resulting in a solution with a concentration of approximately 5 M NaCl. The mixture was heated continuously at 75 °C until the salt completely dissolved. The WPO solution was transferred to the density separator. The WPO beaker was rinsed with distilled water to ensure the complete transfer of any remaining solids. The solids were allowed to settle overnight. An extensive visual inspection of the settled solids was conducted for the purpose of identifying any visible MPs. If any MPs were discovered in the settled solids, they were carefully extracted using forceps, and the residuals were discarded. The supernatants were separated from the floating solids in a clean beaker, and then the supernatant was filtered using

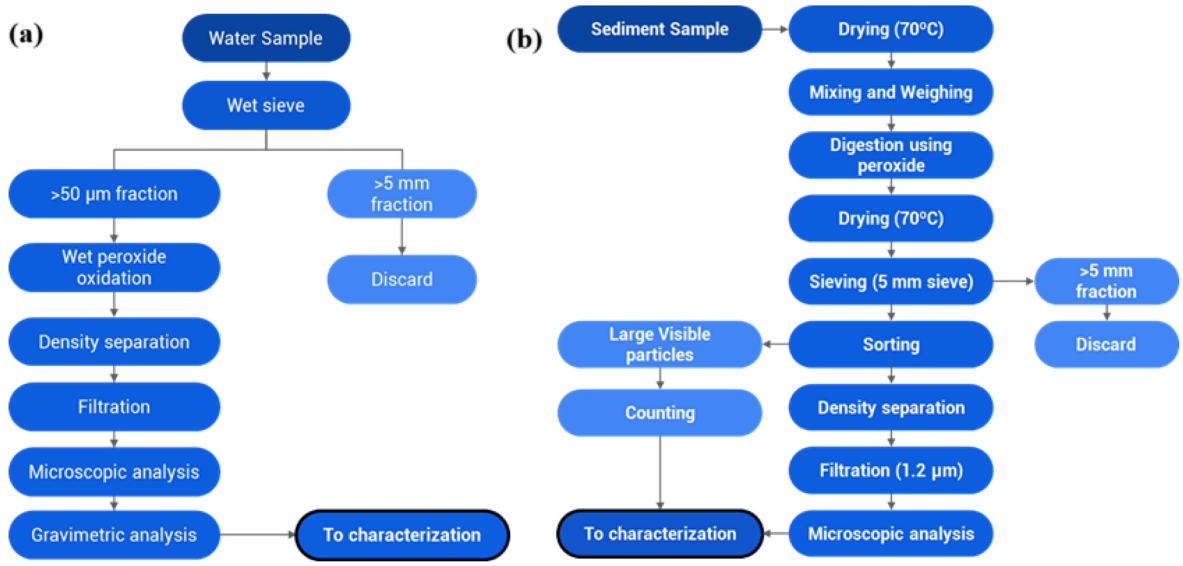

Fig. 2 Block diagram of methods for processing (a) water samples, and (b) sediment samples.

Whatman GF/C filter paper (1.2 μm) with the help of a vacuum pump. The separated MPs were stored in a clean and moisture-free vial. The overall water sample processing method is illustrated in Fig. 2(a).

2.3.2. Sample processing and MPs isolation from the sediment. The sediment samples were dried at 70 °C until a constant weight was achieved. Each sample was homogeneously mixed, and 200 g of dried sample was transferred into a clean glass beaker. 30% H_2O_2 was added to digest organic matter. After digestion, samples were dried again at 70 °C until a constant weight was achieved. Sieving is performed if any visible MPs are observed, and to remove particles larger than 5 mm. Density separation was performed using NaCl solution. The supernatant was allowed to settle for 24 hours, and the upper layer of the solution was filtered with pre-dried Whatman GF/C filter paper (1.2 μm), assisted by a vacuum pump. The filter paper was then rinsed with distilled water. Finally, the filter paper was dried at 40 °C for 24 hours before microscopic inspection. The overall sediment sample processing method is illustrated in Fig. 2(b).

2.4. Visual identification of microplastics

Visible and larger MPs were counted using forceps and a magnifying glass. Smaller MPs were counted using a camera-mounted microscope (Model: Nikon Eclipse E100, magnification: 4×, 10×, 40×, 100×). The filter paper containing MPs was directly placed under a microscope, and the mounted camera was utilized to observe MPs in the filter paper and capture pictures of MPs. Morphological identification followed standardized criteria such as fragments (irregular edges, variable thickness), fibers (elongated cylindrical forms), films (thin flexible sheets), and beads (nearly spherical shapes). The entire quantification procedure was conducted in an enclosed area to prevent sample loss and counting errors, with each sample being counted three times. Visual classifications were systematically validated against polymer groups identified through FTIR analysis of composite samples (Section 2.5). The size and color composition of the MPs were also observed. ImageJ software was utilized for the size measurement of all MPs.

2.5. Characterization of microplastics

Fourier Transform Infrared Spectroscopy (FTIR) was used to determine the type of polymer present in the MPs. For each sample, the entirety of isolated MPs was homogenized and analyzed as a composite to identify dominant polymer groups. Therefore, multiple FTIR measurements (>3 per sample) were performed on homogenized subsamples to ensure comprehensive coverage of polymer groups. The FTIR spectra were recorded for all the samples in the region of 4000–400 cm^{-1} using a Thermo Fisher Scientific Nicolet iS5 FTIR spectrometer. Spectra were collected at 4 cm^{-1} resolution with 32 scans per measurement after automatic background subtraction. The homogenized sample was placed on a diamond crystal to collect the sample spectrum. The collected spectrum is compared to the spectra of various pure polymers to identify the sample content. This approach confirmed that all visually identified particles belonged to polymer groups detected in the sample. The surface morphology of the MPs was evaluated by Scanning Electron Microscopy (SEM) (microscope model: Zeiss EVO18, magnification: 500–11,000×, acceleration voltage: 10 kV). A small, demystified sample was placed on a two-sided conductive carbon-based tape. The carbon tape was then placed in the sample holder. Images of different positions were captured at the micro level. In addition, Energy Dispersive X-ray (EDX) spectroscopy was performed to analyze the elemental composition of the MP surface.

2.6. Microplastics removal using the electrocoagulation process

2.6.1. Electrocoagulation experiment. EC experiments were conducted in an open, undivided, square cell made of a 5 mm

PVC transparent sheet having a cross-section of (14.8 × 14.8) cm^2 with a volume of 4 L. Two aluminum plates were used as electrodes, having a dimension of 13.1 cm × 9.4 cm × 0.15 cm. The electrode spacing was measured to be 11.4 cm. All the experiments were conducted at room temperature. The configuration of EC is represented in Fig. S2.

EC experiment was performed using 2 L of natural river water from the Buriganga and Turag rivers, applying 5, 10, and 15 V. To easily understand the correlation between MP removal efficiency and applied voltage, minimum voltages were applied. A total of six runs were conducted, with three runs utilizing Buriganga river water at voltage levels of 5, 10, and 15 V, and the remaining three runs utilizing Turag river water at the same voltage levels. 67% of the total electrode surface area was immersed in water. This 67% immersion was used to overcome the surging and corrosion of metallic wire under stirred conditions. All experiments were conducted with a consistent stirring rate of 150 rpm using a magnetic stirrer to efficiently distribute the micro-coagulants generated during the process. The 'Dazheng DC Power Supply' converter was used for the power supply.

During the experiment, 20 mL of supernatant was collected into a beaker using a pipette after 5, 10, 15, 20, 30, 45, 60, 75, 90, 120, and 150 minutes. The 20 mL water sample was carefully collected from a depth of 2–3 cm below the water surface to ensure the exclusion of any foam or sludge. The collected supernatants were processed to analyze MP content following the previously mentioned sample processing methods in Section 2.3.1. Then, MPs were counted carefully following the previously mentioned sample processing methods in Section 2.4. Thus, MP contents at 0, 5, 10, 15, 20, 30, 45, 60, 75, 90, 120, and 150 minutes were determined.

After each experiment, the electrodes were immersed in 1 M H_2SO_4 for 5 minutes, abraded with a steel scrubber, followed by sequential washing with tap water and distilled water, and then oven dried at 105 °C. This was performed to remove the passivation layer formed during experimentation.

The MP removal efficiency was calculated to evaluate the treatment performance using the following equation:

$$\%\text{Removal} = \frac{C_0 - C_t}{C_0} \times 100\% \quad (1)$$

where C_0 and C_t were the initial and present values of the MP content.

The changes in pH, dissolved oxygen (DO), total dissolved solids (TDS), total suspended solids (TSS), and electrical conductivity were evaluated using standard methods during the EC process.

2.6.2. Kinetics study. The removal kinetics of MPs using the EC process were studied for both Buriganga river and Turag river samples using zero-order, first-order, and second-order kinetic models. This kinetic analysis was essential to understand the dominant removal mechanism, where second-order kinetics specifically probes aggregation *via* particle–coagulant collisions. The integrated form of expressions for zero-order, first-order, and second-order kinetic models is illustrated in eqn (2)–(4), respectively.

$$C_0 - C_t = k_0 t \quad (2)$$

$$\ln\left(\frac{C_0}{C_t}\right) = k_1 t \quad (3)$$

$$\frac{1}{C_t} - \frac{1}{C_0} = k_2 t \quad (4)$$

where t is the total EC run time and k_0 (MPs per L per min), k_1 (min^{-1}), and k_2 (L per MPs per min) represent the rate constants of zero, first, and second-order kinetic models, respectively.

2.7. Spatial clustering and risk assessment

To analyze spatial patterns of microplastic pollution, hierarchical cluster analysis (HCA) was performed on MP abundance and weight data from all sampling stations. The analysis employed Euclidean distance to quantify dissimilarities between samples and Ward's linkage method to minimize within-cluster variance, with separate analyses conducted for water and sediment samples in both rivers during dry and wet seasons. This clustering approach allowed identification of stations with similar pollution characteristics while preserving the quantitative relationships between sites.

To assess the level of MP pollution in these rivers, the pollution load index (PLI) method is employed. Tomlison *et al.* (1980) proposed this method to assess the ecological risk, and it is widely used for aquatic environments.[49] The assessment model is as follows:[49,50]

$$\text{CF}_i = \frac{C_i}{C_{0i}} \quad (5)$$

$$\text{PLI} = \sqrt{\text{CF}_i}\text{PLI}_{\text{zone}} = \sqrt[n]{\text{PLI}_1\text{PLI}_2\text{PLI}_3\ldots\text{PLI}_n} \quad (6)$$

CF_i is the quotient of the concentration (C_i) of microplastics at each sampling site and the minimum microplastic concentration (C_{0i}). C_{0i} is a defined value for a water or sediment sample of a river.

2.8. Quality assurance/quality control

To minimize sample contamination during the MPs analysis procedure, glass products were prioritized over plastic products throughout the whole process. An amber glass bottle was utilized for storing water samples, as it provides excellent UV protection.[51] Nitrile gloves were consistently worn during experiments, and all laboratory procedures were carried out on clean benches. Procedural blanks were implemented for all sample types: (1) Water blanks ($n = 3$ per batch) using filtered DI water processed identically to samples showed negligible contamination, and (2) sediment blanks ($n = 3$ per batch) using pre-combusted commercial sand (450 °C, 4 h) yielded 30.2 ± 1.5 particles per kg. These blank values were subtracted from the corresponding sample abundances. The lab desk was cleaned using 70% alcohol and distilled water regularly. All apparatus utilized in this study were thoroughly cleaned with distilled water and wrapped in aluminum foil to prevent contamination. To avoid melting any MPs, all samples were dried at a temperature range of 70–80 °C. Temperature was controlled during

digestion using a water bath to prevent the melting or loss of MPs during digestion. The density separator was thoroughly washed several times to collect all the MPs and minimize sample loss. Additionally, each sample was covered with aluminum foil after each processing step to minimize air contamination and potential sample loss. Each sample was counted three times to reduce quantification errors. The quantification was conducted in a separate room to minimize the number of individuals in the laboratory. The electric fan and air conditioner were turned off, and a mask was worn during quantification to minimize sample loss *via* airflow. While formal recovery tests were not conducted, the triplicate processing of all samples and consistent handling protocols minimized particle loss variability. In addition, it has to be acknowledged that particles <50 μm may be underrepresented due to the sampling net pore size used in this study, and absolute abundances should be interpreted as conservative estimates.

2.9. Data analysis

All analytical and statistical analyses were performed using Microsoft Excel 2016. Hierarchical cluster analysis (HCA) was conducted in R version 4.3.2 (R Core Team, 2023) within the RStudio integrated development environment (version 2023.09.01; RStudio Team, 2023). Graphical visualizations were generated using Origin Pro 2018.

3 Results and discussion

3.1. Quantification of microplastics

The quantification of microplastics (MPs) in the Buriganga and Turag rivers revealed significant spatial and seasonal variations in pollution levels. As shown in Tables S1, S2, and Fig. 3, the Buriganga River exhibited substantially higher MP concentrations compared to the Turag River, with sediment samples containing markedly greater quantities than water samples across both rivers. This observation suggests that riverbank sediments serve as important sinks for MP accumulation in these aquatic systems.

Seasonal analysis demonstrated pronounced differences in MP abundance between dry and wet periods in the Buriganga River. During the dry season (January–March), water samples contained 26.98 ± 0.15 to 374.84 ± 18.74 MPs per L, while sediment samples ranged from 11 360 ± 1135 to 134 330 ± 5275 MPs per kg. These values decreased significantly during the wet

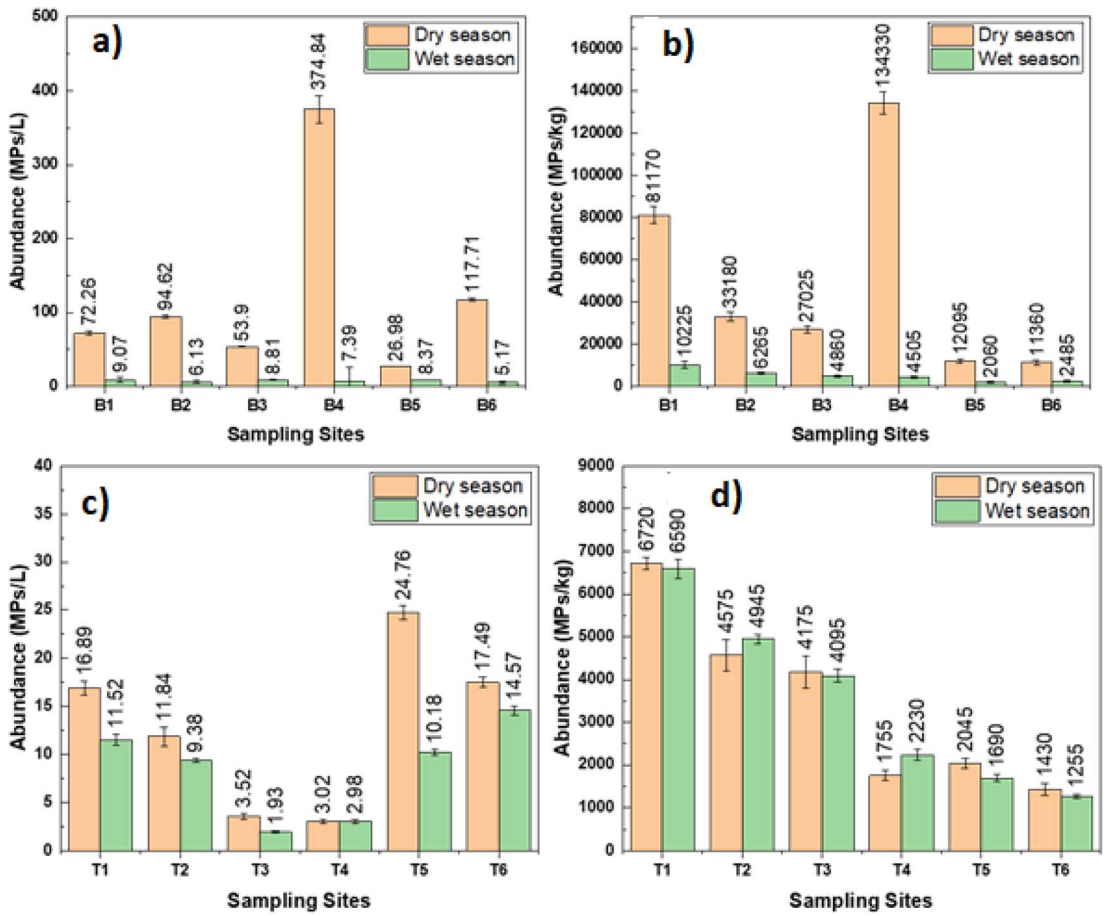

Fig. 3 Seasonal variations of MP abundance in the Buriganga and Turag rivers. (a) Water samples in Buriganga river, (b) sediment samples in Buriganga river, (c) water samples in Turag river, (d) sediment samples in Turag river.

season (July–September), with water concentrations falling to 5.17 ± 0.16 to 9.07 ± 0.46 MPs per L and sediment loads reducing to 2060 ± 455 to 10 225 ± 1600 MPs per kg. The highest contamination levels were consistently observed at station B4 (Chandir Ghat), a known center for plastic recycling activities, where direct handling of plastic waste was visibly evident during sampling (Fig. S3 and S4).

In contrast, the Turag River showed less dramatic seasonal fluctuations. Dry season water samples contained 3.02 ± 0.19 to 24.76 ± 0.71 MPs per L, decreasing to 1.93 ± 0.11 to 14.57 ± 0.44 MPs per L during wet periods. Sediment MP concentrations remained relatively stable between seasons, ranging from 1430 ± 140 to 6720 ± 145 MPs per kg in the dry season and 1255 ± 45 to 6590 ± 230 MPs per kg under wet conditions. The elevated MP levels at station T5 may be attributed to its location at the confluence of two tributaries, where hydrodynamic processes likely enhance particle accumulation.

Morphological characterization identified three predominant MP types: fragments, fibers, and films (Fig. 4).

Size distribution analysis revealed that particles smaller than 300 μm constituted the most abundant fraction across all samples, representing 60.7–75.5% of MPs in the Turag River and 32.6–42.7% in the Buriganga River (Fig. 5 and 6). This size distribution pattern is consistent with the progressive fragmentation of larger plastic debris in aquatic environments. Larger MPs (3–5 mm) were more prevalent in Buriganga samples, potentially reflecting more recent inputs from point sources.

Color analysis showed white MPs to be dominant (26–35% of total particles), followed by black and brown/red particles (Fig. 7 and 8). The color distribution varied between rivers, with transparent MPs being twice as common in the Turag (9.5–12.5%) compared to the Buriganga (5–7%). These differences likely reflect variations in the sources and types of plastic waste entering each river system. The predominance of white and black particles correlates well with the colors commonly used in packaging materials and textile fibers, which represent major components of urban plastic waste.

Substantial disparity in MP pollution between the two rivers can be attributed to several factors. The Buriganga flows through more densely populated and industrialized areas of Dhaka, receiving greater quantities of plastic waste from both municipal and industrial sources. Additionally, its position downstream of the Turag means it accumulates pollutants transported from upstream areas. The Turag's relatively lower MP levels may reflect its passage through less urbanized zones and the presence of fewer direct waste input sources along its course.

3.2. Polymer type of microplastics

The polymer composition of microplastics was determined through FTIR spectral analysis (Fig. 9 and S5), revealing polyethylene (PE) and polypropylene (PP) as the dominant polymer types across both rivers. These accounted for 92% of water samples and 96% of sediment samples, with polystyrene (PS) appearing less frequently (8% in water, 4% in sediment). The characteristic peaks of PE were identified at 2914, 2847, 1470, 1377, and 717 cm^{-1}, corresponding to CH_2 stretching and bending vibrations.[52] PP showed distinct peaks at 2924 cm^{-1}

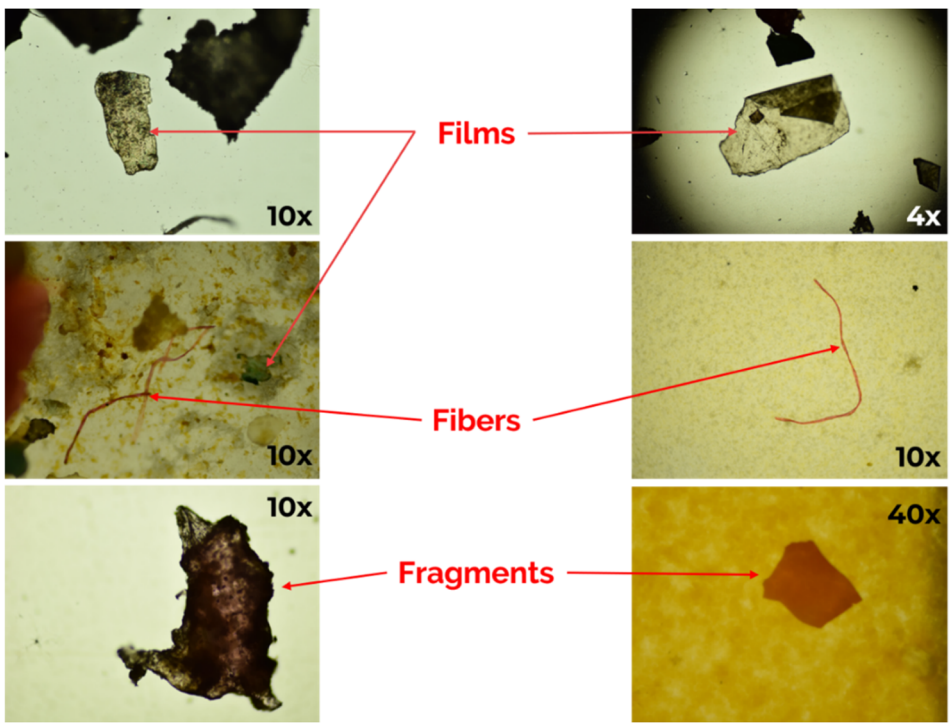

Fig. 4 Microscopic images of MPs observed from the Buriganga and Turag Rivers.

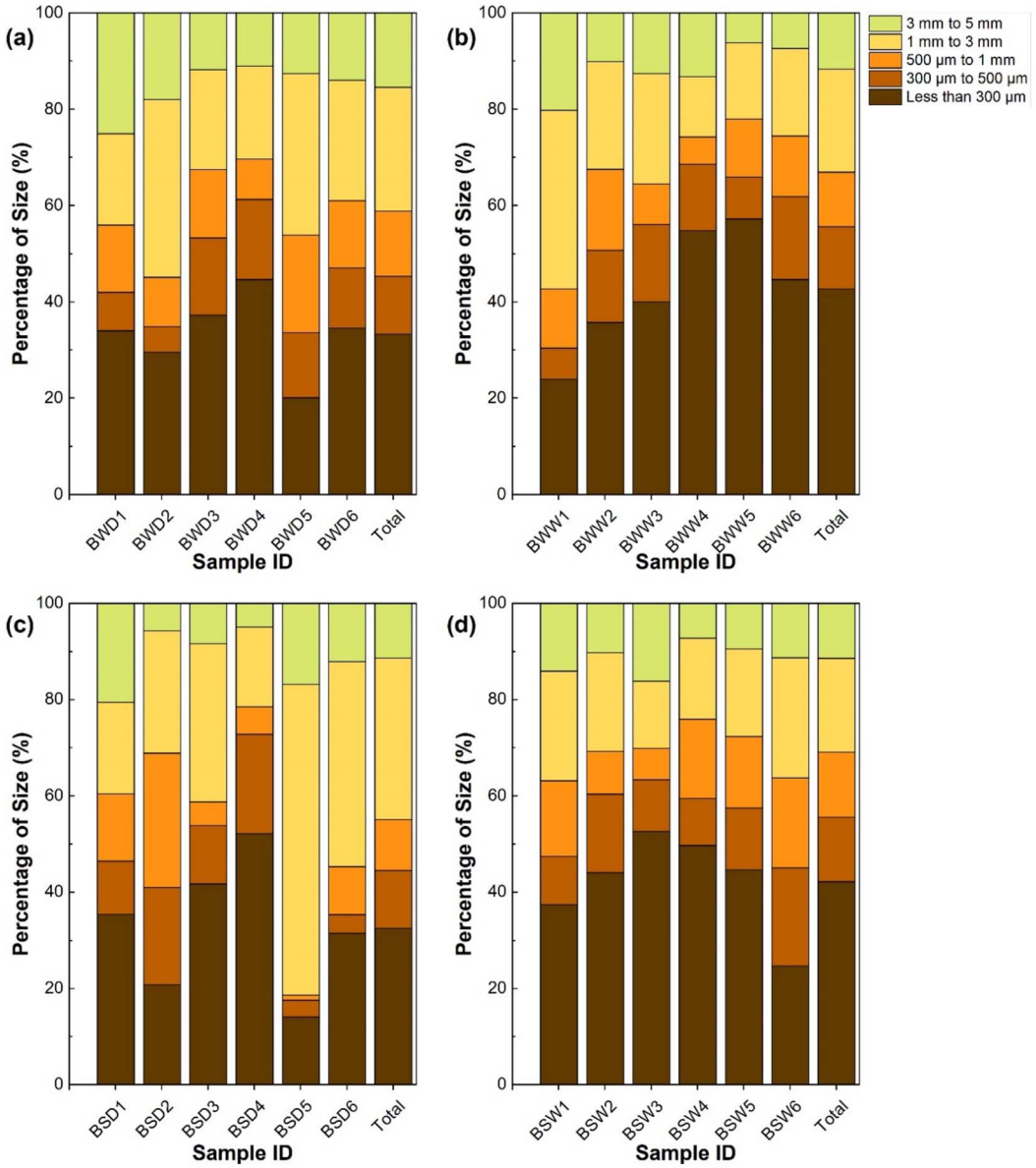

Fig. 5 Size composition of MPs in Buriganga river samples (a) dry season water samples; (b) wet season water samples; (c) dry season sediment samples; (d) wet season sediment samples.

(C–H stretching) and 1431 cm^{-1} (C–C stretching),[53] while PS was identified by aromatic C=C stretches at 1601 cm^{-1} and 1440 cm^{-1}.[54] The polymer distribution varied spatially, with PE predominating near plastic recycling sites like Chandir Ghat (B4), while PP was more common near textile industries along the Turag. PS appeared primarily in urban centers, suggesting different pollution sources. One notable finding was the co-occurrence of all three polymers at station TWD3, indicating mixed contamination at this location. While this analysis provides robust identification of major polymer types, the NaCl density separation method may have limited detection of higher-density polymers like PVC and PET,[55–57] suggesting that the actual polymer diversity in these rivers could be greater than reported. This consideration is particularly relevant for the complex waste streams of Dhaka, where multiple plastic types are present. The complete polymer distribution across sampling sites is detailed in Table S3, with characteristic FTIR peaks summarized in Table 2.

3.3. SEM analysis of microplastics

Fig. 10 presents SEM images of fiber-type microplastics from the Buriganga and Turag rivers, revealing substantial morphological variations with significant environmental implications. Entangled polymer fibers in Fig. 10(a) and (b) correspond to the findings by Prajapati *et al.* (2021), where complex aggregation complicates accurate MP quantification through particle entrapment. In contrast, Fig. 10(c) and (e) exhibit smoother

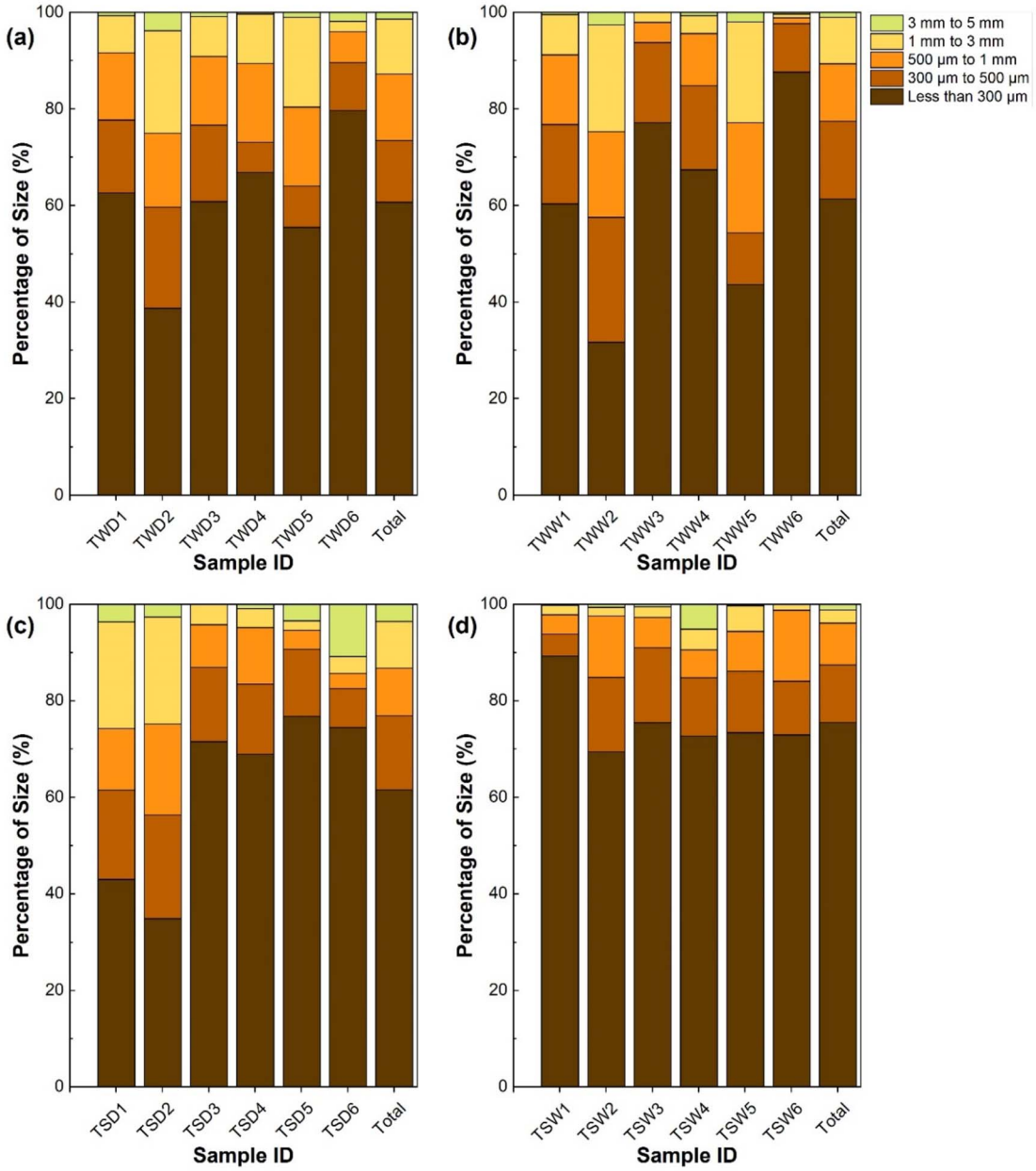

Fig. 6 Size composition of MPs in Turag river samples (a) dry season water samples; (b) wet season water samples; (c) dry season sediment samples; (d) wet season sediment samples.

fibers with minimal surface adherents, suggesting recent environmental introduction from textile effluents or municipal waste discharge. Fig. 10(d) demonstrates fibers with adhered particulate matter, consistent with Tsering *et al.* (2021)[63] regarding the role of MPs as carriers for co-pollutants. Evidence of progressive weathering in Fig. 10(g) and (h), revealed through cracks and flakes, aligns with mechanical fragmentation mechanisms described by Ainali *et al.* (2021).[64] Complementary analysis in Fig. S6 shows surface fractures in Fig. S6(a) and (b), indicating advanced weathering stages[65,66] that enhance contaminant adsorption capacity. Fig. S6(g) displays morphologically intact particles, implying recent deposition,[67] while thin-edge artifacts in Fig. S6(b) result from electron beam penetration during SEM imaging. Critically, adherent microparticles in Fig. S6(a), S8(c), (f), and (h) confirm MPs as substrates for heavy metal accumulation.[62,63,65,66] These morphological distinctions reflect source-specific patterns where textile-dominated inputs in the Buriganga contrast with the mixed anthropogenic origins in Turag,[24] degradation timelines affecting contaminant bioavailability,[68] and region-specific pollution drivers necessitating tailored remediation strategies for waste management challenges in Dhaka.[19] The pervasive surface alterations underscore the possible evolution of MPs into chemically active environmental vectors during aging processes.

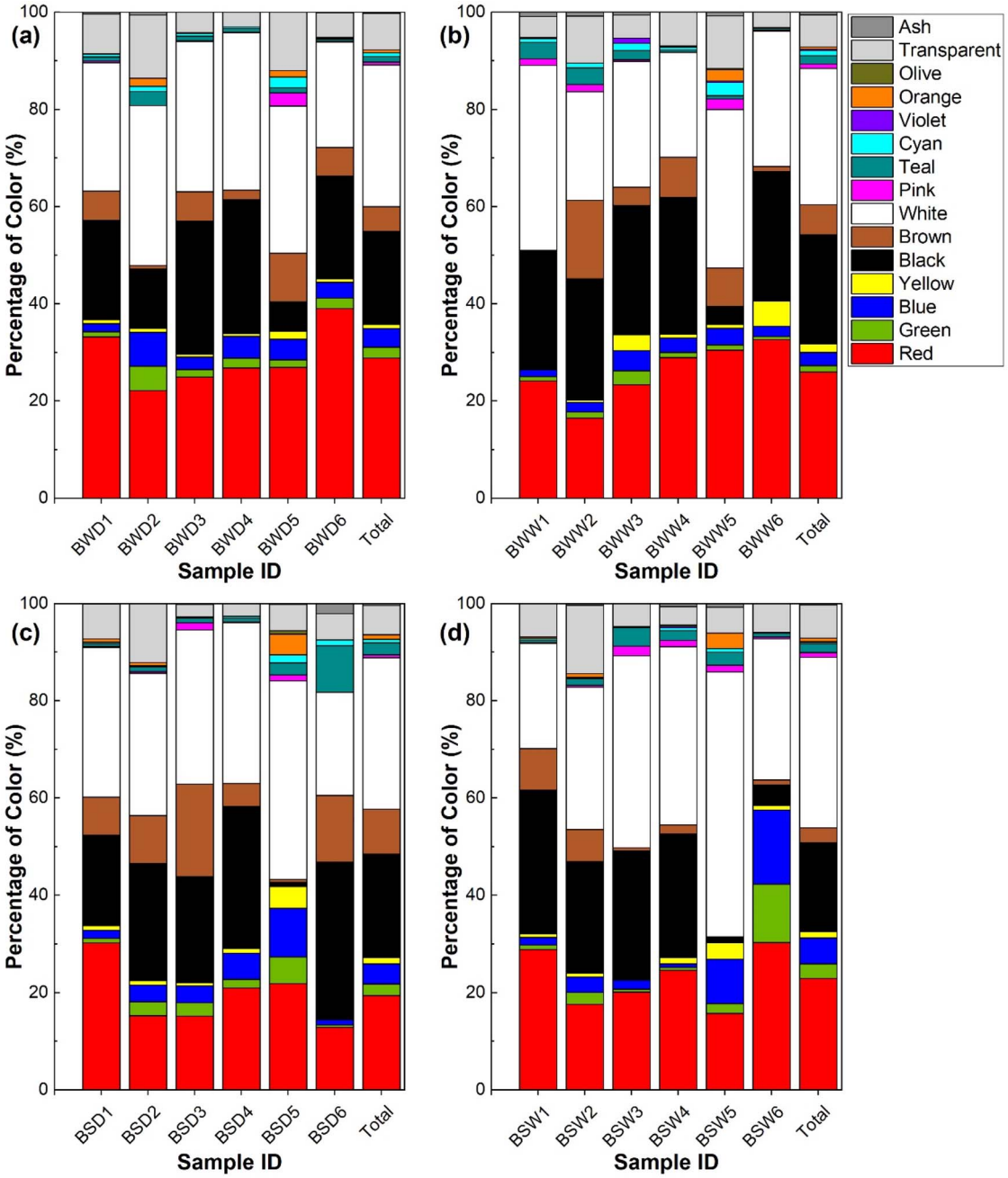

Fig. 7 Color composition of MPs in Buriganga river samples (a) dry season water samples; (b) wet season water samples; (c) dry season sediment samples; (d) wet season sediment samples.

3.4. Presence of heavy metals in microplastics

Energy-dispersive X-ray (EDX) analysis revealed substantial adsorption of heavy metals onto microplastics (MPs) from both rivers, with Table 3 (Buriganga) and Table S4 (Turag) quantifying elemental compositions. MPs carried notable concentrations of toxic metals, including Cr (up to 6.53 wt% at BSD4), Cd (up to 2.08 wt% at BSD4), Pb (up to 3.56 wt% at BSD4), and Hg (up to 5.01 wt% at BSW6), aligning with documented heavy metal pollution in these waterways.[26,71] These findings confirm the role of MPs as pollutant carriers, particularly at site B4 (Chandir Ghat) near recycling facilities, where exceptionally high metal levels corresponded with local industrial activities (Table 1).

The adsorption mechanisms involve both physical and chemical pathways. Surface weathering features observed through SEM, including fractures, flakes, and cavities, increase available surface area,[68] facilitating metal deposition. Concurrently, electrostatic interactions and surface complexation enhance binding affinity for cationic metals like Pb^{2+} and Cd^{2+},[68–70] which creates persistent composite pollutants, as both

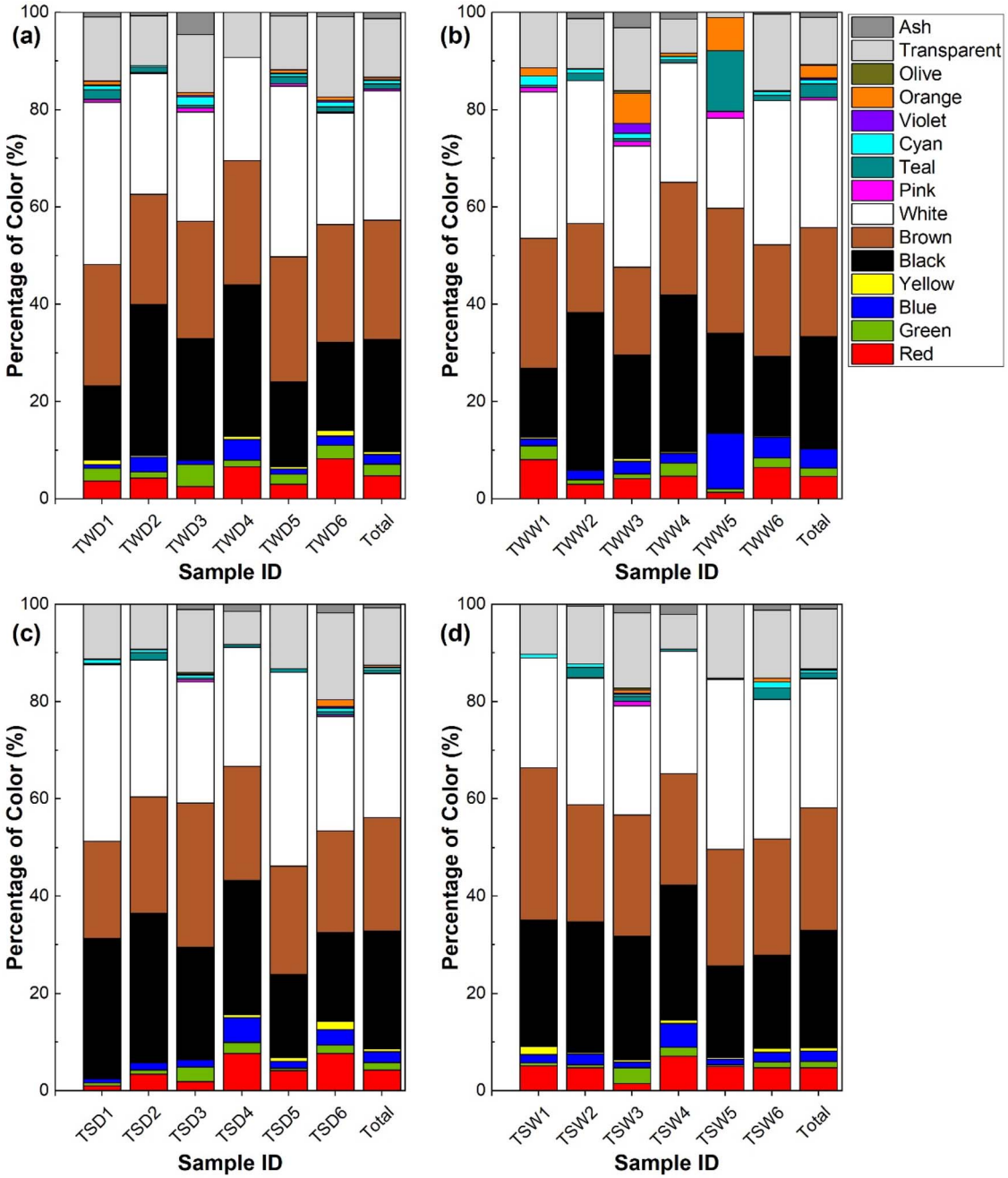

Fig. 8 Color composition of MPs in Turag river samples (a) dry season water samples; (b) wet season water samples; (c) dry season sediment samples; (d) wet season sediment samples.

MPs and heavy metals resist degradation and accumulate in ecosystems for decades. Critically, co-existence amplifies toxicity through combined effects, with studies showing elevated bioaccumulation when metals bind to MPs.[72]

These metal-bound MPs pose dual threats, *e.g.*, ecological risks through trophic transfer when ingested by aquatic organisms,[15,17] and human health impacts *via* contaminated fisheries, where Cd/Pb exposure correlates with renal impairment and neurotoxicity.[72] The spatial metal distribution mirrored river pollution gradients, with Buriganga samples exhibiting consistently higher metal loads than Turag, corresponding to its greater industrial burden.[24,29] These results highlight the urgency of source-specific interventions targeting industrial discharges in critical zones like Chandir Ghat.

3.5. Performance of electrocoagulation

Electrocoagulation (EC) treatment of natural river water from the Buriganga and Turag rivers achieved high microplastic (MP) removal efficiencies, which increased with both applied voltage and treatment duration (Fig. 11).

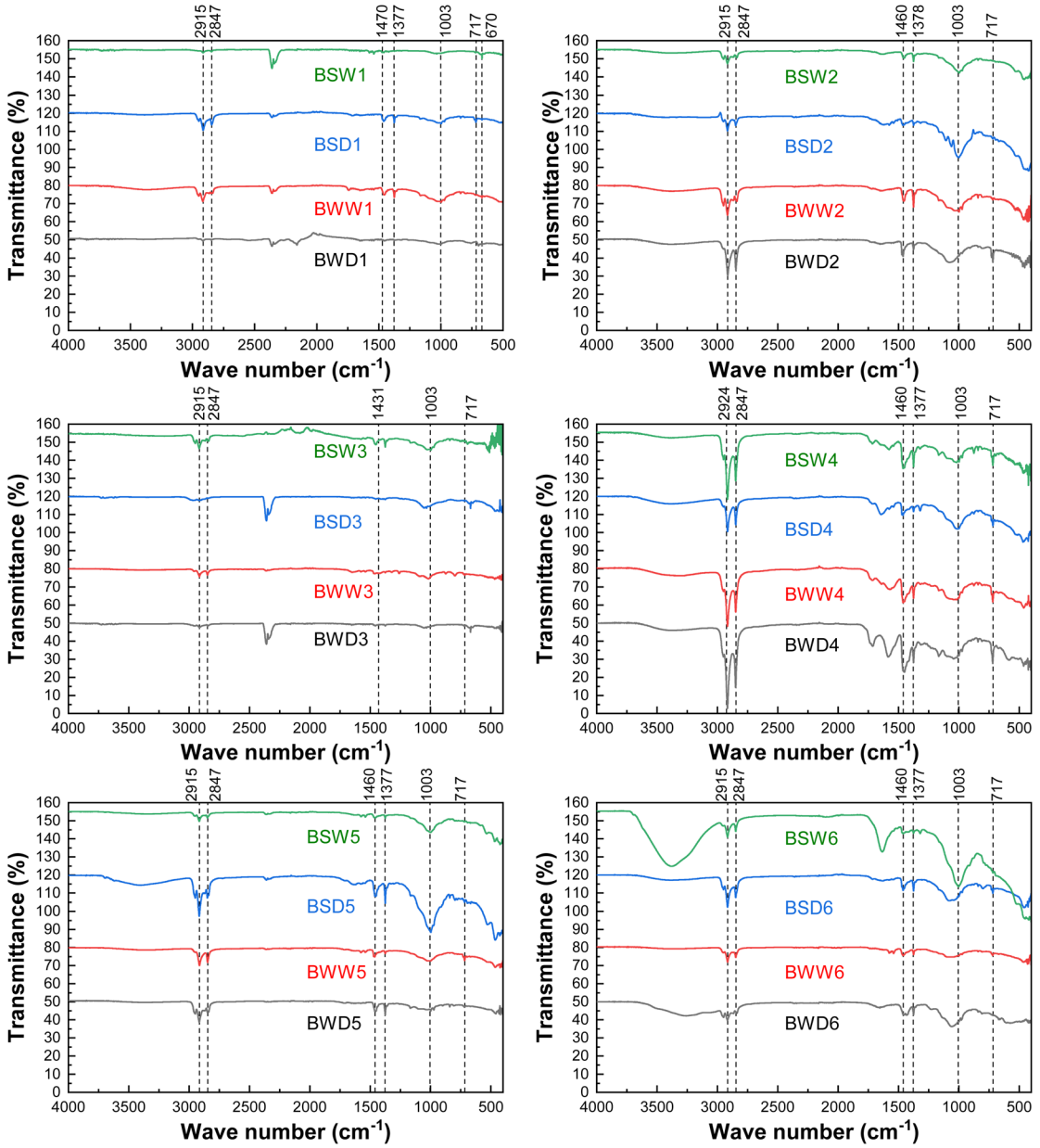

Fig. 9 FTIR spectra of collected samples of Buriganga River (BWD: Buriganga water sample in dry season, BSD: Buriganga sediment sample in the dry season, BWW: Buriganga water sample in the wet season, BSW: Buriganga sediment sample in the wet season).

Table 2 Polymers observed in this study and their characteristic peaks[52–54,58–61]

Polymer	Key functional groups/bonds	Characteristic FTIR peaks (cm^{-1})	Peak assignments
PE	C–H (alkane), C–C backbone	2915, 2848	Asymmetric and symmetric CH_2 stretching
		1470	CH_2 bending
		~1377	CH_3 umbrella mode
		~720	CH_2 rocking
PP	C–H (alkane), –CH_3 side groups	~2950, 2916, 2838	CH_3 asymmetric and symmetric stretching
		~1431 (between 1465 and 1365)	C–C stretching band peak
		~1003 (between 1000 and 900)	CH_3 bond oscillation band peak
PS	Aromatic C=C, C–H (alkane), aromatic ring	3050	Aromatic C–H stretching
		2840	C–H stretching
		1600, 1440	Aromatic C=C stretching
		698–750, 530	Aromatic C–H out-of-plane bending

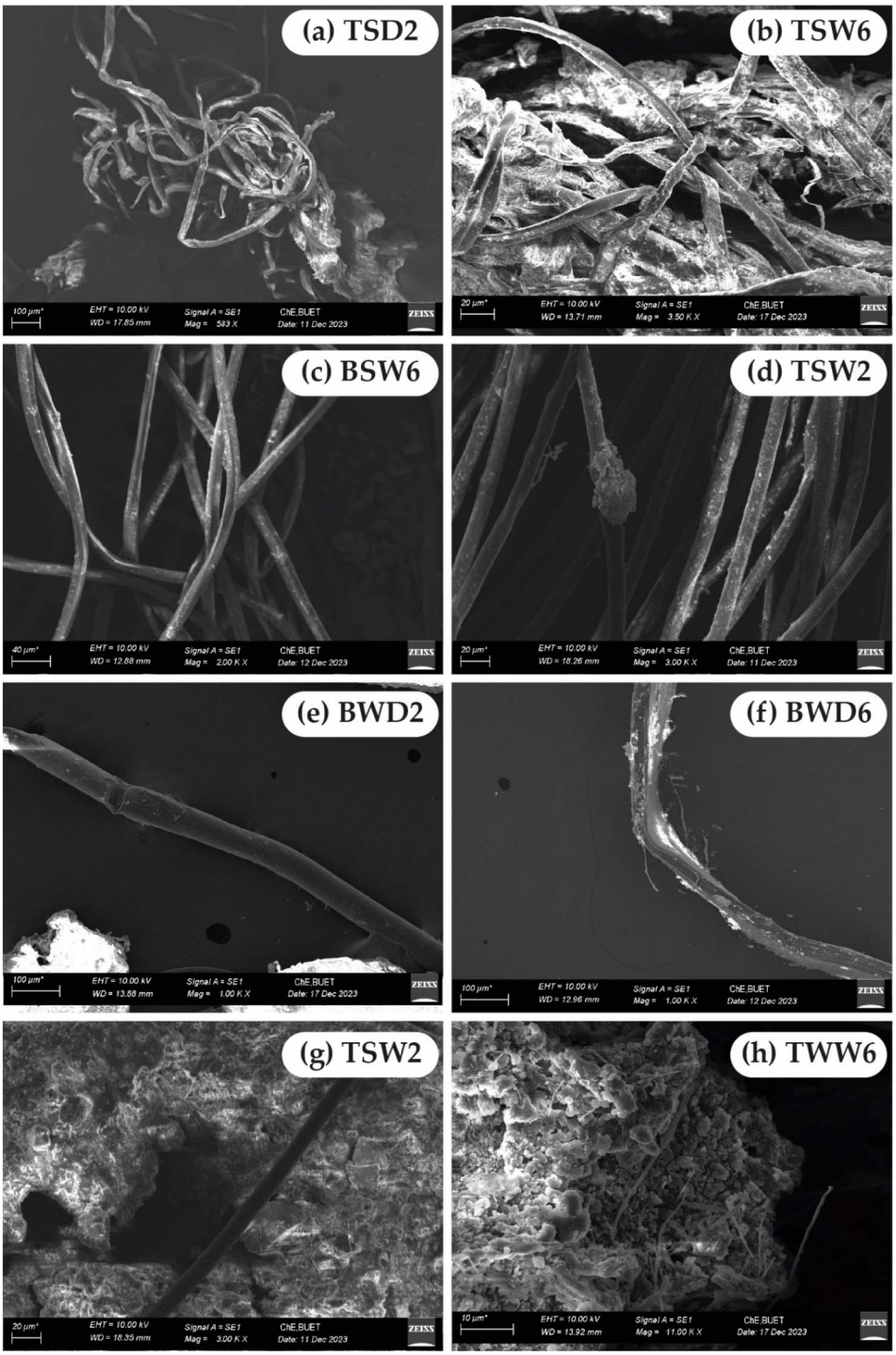

Fig. 10 Selected SEM images of collected samples (fibers).

Maximum removal efficiencies of 99.06% for Buriganga water and 99.49% for Turag water were achieved at 15 V after 150 minutes, while 60 minutes treatments at this voltage resulted in 96.24% and 97.69% removal, respectively. This voltage-dependent performance results from enhanced aluminum hydroxide ($Al(OH)_3$) coagulant formation through electrochemical reactions (eqn (7)–(11)),[33] where higher voltages accelerate Al^{3+} generation from the anode.

$$M_{(s)} \rightarrow M^{n+}_{(aq)} + ne^- \quad (7)$$

$$2H_2O_{(l)} \rightarrow 4H^+_{(aq)} + O_{2(g)} + 4e^- \quad (8)$$

$$M^{n+}_{(aq)} + ne^- \rightarrow M_{(s)} \quad (9)$$

Table 3 Elemental composition (wt%) of MPs in different samples of the Buriganga river

Element	BWD2	BWW2	BSD2	BSW2	BWD4	BWW4	BSD4	BSW4	BWD6	BWW6	BSD6	BSW6
C	86.49	61.51	73.81	73.24	67.02	48.83	39.2	53.34	86.9	75.97	78.91	73.1
N	2.92	6.19	5.88	5.91	3.7	3.53	3.12	4.83	4.48	4.37	3.45	4.14
O	6.37	24.56	15.46	16.45	19.86	34.96	39.8	33.3	4.3	13.19	9.7	12.03
F	0.05	1.35	0.79	0.74	3.42	6.99	3.85	2.93	0.04	0.55	0.43	0.52
S	0	0	0	0	0.01	0.01	0.01	0.01	0	0	0	0
Cl	0.13	0.23	0.08	0.15	1.28	0.16	1.75	0.62	0.06	0.09	0.18	0.23
Cr	0.26	0.33	0.33	0.19	2.74	2.72	6.53	0	0.32	0.25	0.42	0.62
Mn	0.21	0.34	0.28	0.22	0	0	0	0.02	0.31	0.17	0.37	0.44
Fe	0.34	1.8	0.85	0.6	0	0.01	0.04	0	0.28	0.85	0.68	0.75
Co	0.18	0.27	0.2	0.14	0	0	0	0.01	0.24	0.21	0.47	0.31
Ni	0.22	0.28	0.24	0.24	0.02	0	0	0	0.19	0.15	0.51	0.4
Pd	0.22	0.34	0.28	0.21	0.01	0	0.01	0	0.18	0.27	0.39	0.4
Cd	0.14	0.19	0.13	0.1	1.00	1.16	2.08	1.01	0.1	0.11	0.07	0.18
Sn	0.17	0.15	0.12	0.07	0	0.01	0.01	0.01	0.09	0.15	0.11	0.38
Sb	0.2	0.33	0.24	0.25	0.01	0.01	0.03	0.01	0.23	0.27	0.57	1.36
Hg	2.01	2.07	1.21	1.4	0.01	0.01	0.01	0.01	2.23	3.34	3.59	5.01
Pb	0.08	0.06	0.1	0.09	0.92	1.6	3.56	2.1	0.05	0.06	0.15	0.14
Cu	0	0	0	0	0	0	0	1.8	0	0	0	0

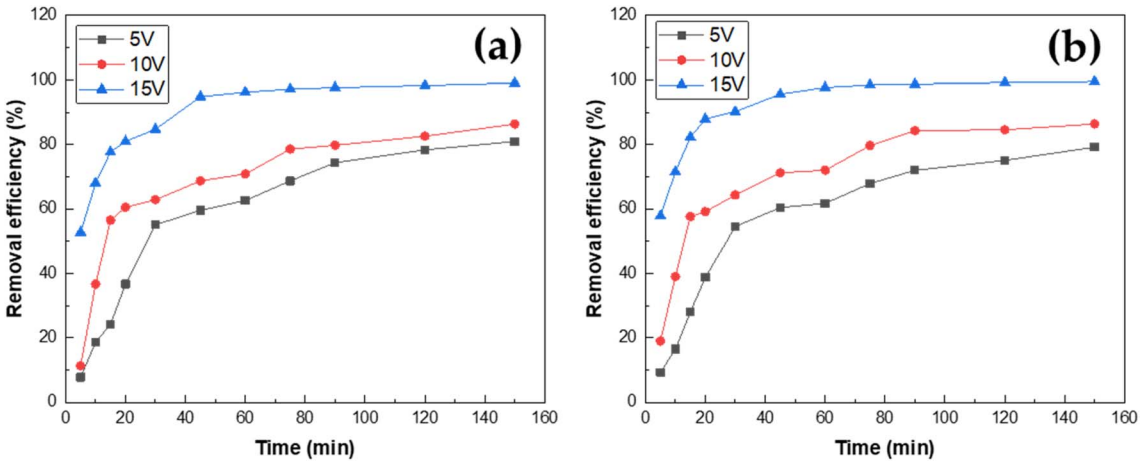

Fig. 11 Removal efficiency of MPs from river water. (a) Buriganga river water and (b) Turag river water.

$$2H_2O_{(l)} + 2e^- \rightarrow 2OH^-_{(aq)} + H_{2(g)} \quad (10)$$

$$M^{n+}_{(aq)} + nOH^-_{(aq)} \rightarrow M(OH)_{n(s)} \quad (11)$$

The coagulation process was confirmed by a progressive pH increase (Fig. S7), indicating $Al(OH)_3$ accumulation, and decreased dissolved oxygen (Fig. S8) from oxygen evolution during electrolysis.

EC simultaneously reduced other pollutants, with conductivity and total dissolved solids (TDS) in Turag water decreasing from 572 μS cm^{-1} to <7 μS cm^{-1} and 286 mg L^{-1} to <4 mg L^{-1} within 5 minutes (Table S5). Similarly, total suspended solids (TSS) decreased by 93% on average after 150 minutes (Table S6). These efficiencies compare favorably with the literature for synthetic systems (Table S7), such as 96.3% removal of PVC and PE using Fe–Al electrodes in 120 minutes[38] and >99% removal in synthetic wastewater within 60 minutes,[33] despite treating natural water containing diverse MPs rather than single-polymer suspensions. However, the >99% efficiency represents total suspended solid reduction rather than MP-specific elimination, as post-floc characterization was not conducted, a limitation for future studies to address through polymer-specific analysis.

3.6. Kinetics study

The reaction kinetics of microplastic (MP) removal by electrocoagulation were systematically evaluated using zero-order, first-order, and second-order models applied to experimental data from both rivers. Fig. 12 and Table S8 demonstrate the consistent superiority of the second-order kinetic model across all experimental conditions, with R^2 values exceeding 0.98 for both rivers at 15 V compared to ≤0.91 for alternative models. For instance, Buriganga River samples at 5 V showed R^2 values

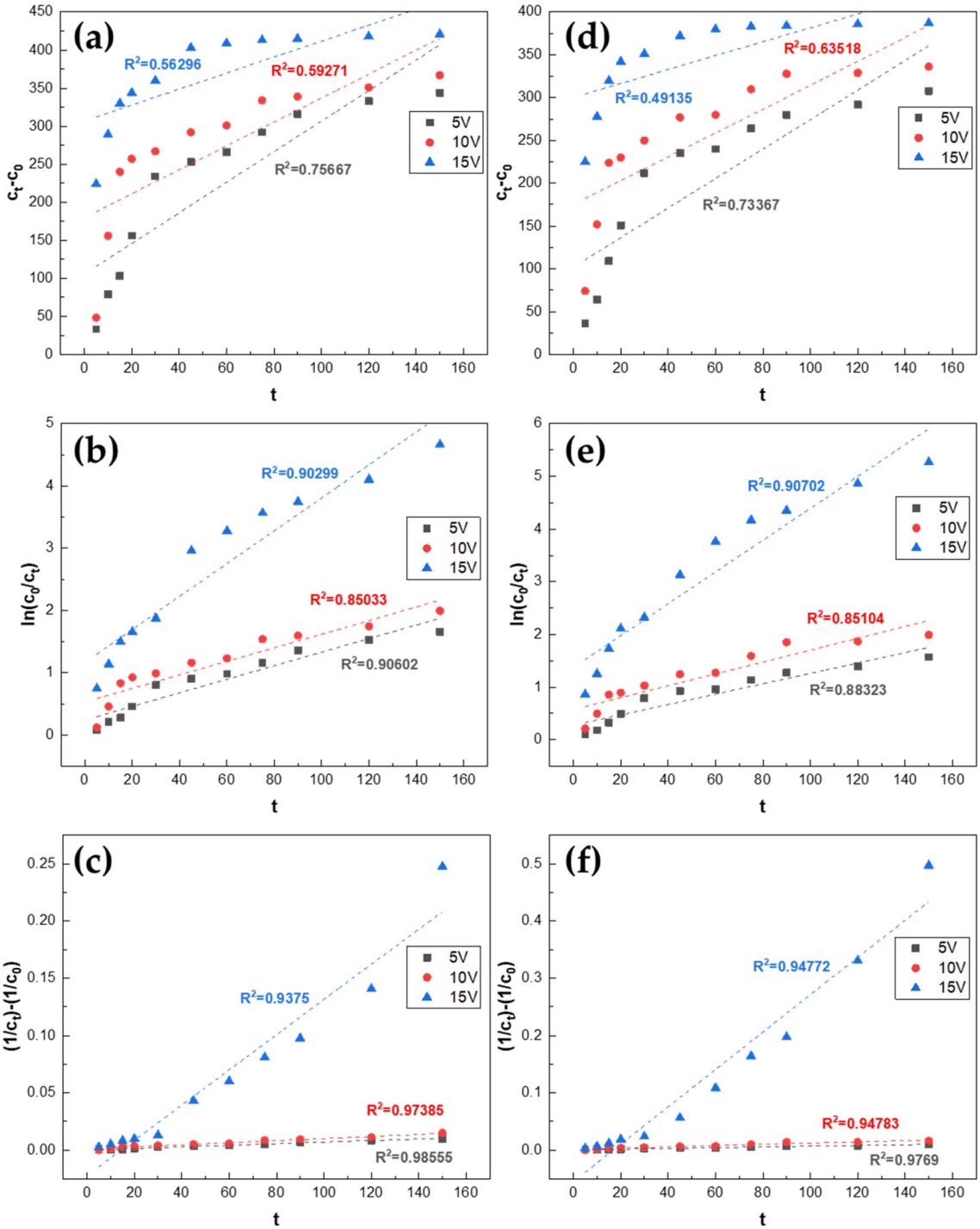

Fig. 12 Reaction kinetics of MPs removal using the EC process: (a) Buriganga sample-zero order, (b) Buriganga sample-first order, (c) Buriganga sample-second order, (d) Turag sample-zero order, (e) Turag sample-first order, and (f) Turag sample-second order.

of 0.76 (zero-order), 0.91 (first-order), and 0.99 (second-order), while Turag River samples exhibited similar trends (0.73, 0.88, and 0.98, respectively). This consistent pattern confirms that MP removal occurs primarily through bimolecular collisions between MPs and aluminum hydroxide flocs ($Al(OH)_3$),[33,46] where particle–coagulant interactions constitute the rate-limiting step rather than surface reactions or unimolecular decay.[38,45]

Critically, second-order rate constants (k_2) increased substantially with applied voltage: from 6.91×10^{-5} to 1.54×10^{-3} L per MPs per min in Buriganga water and 6.46×10^{-5} to 3.26×10^{-3} L per MPs per min in Turag water as voltage escalated from 5 V to 15 V. This voltage-dependence directly

correlates with the electrochemical fundamentals of EC, where higher voltages accelerate Al^{3+} generation (eqn (7)), increasing coagulant availability and collision frequency.[46] The high k_2 value at 15 V mechanistically explains the efficiency improvements documented in Section 3.5, confirming 15 V as optimal for urban river treatment. These kinetics provide critical insights for scaling EC systems in pollution hotspots like Dhaka, where collision-driven removal mechanisms offer energy-efficient solutions for complex particulate mixtures.

3.7. Hierarchical cluster analysis (HCA) and risk assessment

Hierarchical cluster analysis (HCA) of microplastic abundance and weight data identified distinct spatial groupings across sampling stations for both rivers and seasons (Fig. 13 and 14). Water samples from the Buriganga River during the dry season formed three clusters: Cluster 1 (BWD1, BWD3, BWD5), Cluster 2 (BWD2, BWD6), and Cluster 3 (BWD4). In the wet season, clusters shifted to Cluster 1 (BWW1), Cluster 2 (BWW2, BWW4, BWW6), and Cluster 3 (BWW3, BWW5). Similar clustering patterns emerged for Turag River water samples: dry season Cluster 1 (TWD1, TWD2), Cluster 2 (TWD5, TWD6), Cluster 3 (TWD3, TWD4); wet season Cluster 1 (TWW1, TWW5, TWW2), Cluster 2 (TWW6), and Cluster 3 (TWW3, TWW4).

Sediment analysis revealed parallel groupings. Buriganga sediments clustered as dry season Cluster 1 (BSD1, BSD4), Cluster 2 (BSD2), and Cluster 3 (BSD3, BSD5, BSD6); wet season Cluster 1 (BSW1), Cluster 2 (BSW2, BSW3, BSW4), and Cluster 3 (BSW5, BSW6). Turag sediments grouped as dry season Cluster 1 (TSD1, TSD2, TSD3), Cluster 2 (TSD6), Cluster 3 (TSD4, TSD5); wet season Cluster 1 (TSW1, TSW2), Cluster 2 (TSW3, TSW4), and Cluster 3 (TSW5, TSW6).

These spatial patterns consistently highlighted pollution hotspots, with Chandir Ghat (BWD4/BSD4) forming isolated clusters in the Buriganga during dry seasons, confirming its status as a microplastic pollution hotspot. Wet season clusters showed greater station consolidation, particularly in Turag water samples, indicating hydrological homogenization during monsoon periods.

The Pollution Load Index (PLI) was calculated for all samples using minimum observed microplastic concentrations as baseline values (C_{0i}).[73] In this study, the C_{0i} values for the Buriganga River were 517 MP/100 L for water samples and 2060 MP per kg for sediment samples. For the Turag River, the corresponding values were 193 MP/100 L and 1255 MP per kg for water and sediment, respectively.

PLI values across sampling sites (Fig. 15 and Table S9) indicate significant seasonal variations. The Buriganga River exhibited peak PLI values during the dry season (water: 4.11; sediment: 4.02), with a substantial decrease in both matrices during the wet periods. All values remained below the Risk Level I threshold (PLI < 10), and sediments consistently maintained this classification. Turag exhibited distinct patterns: sediment PLI remained constant (1.53) year-round,

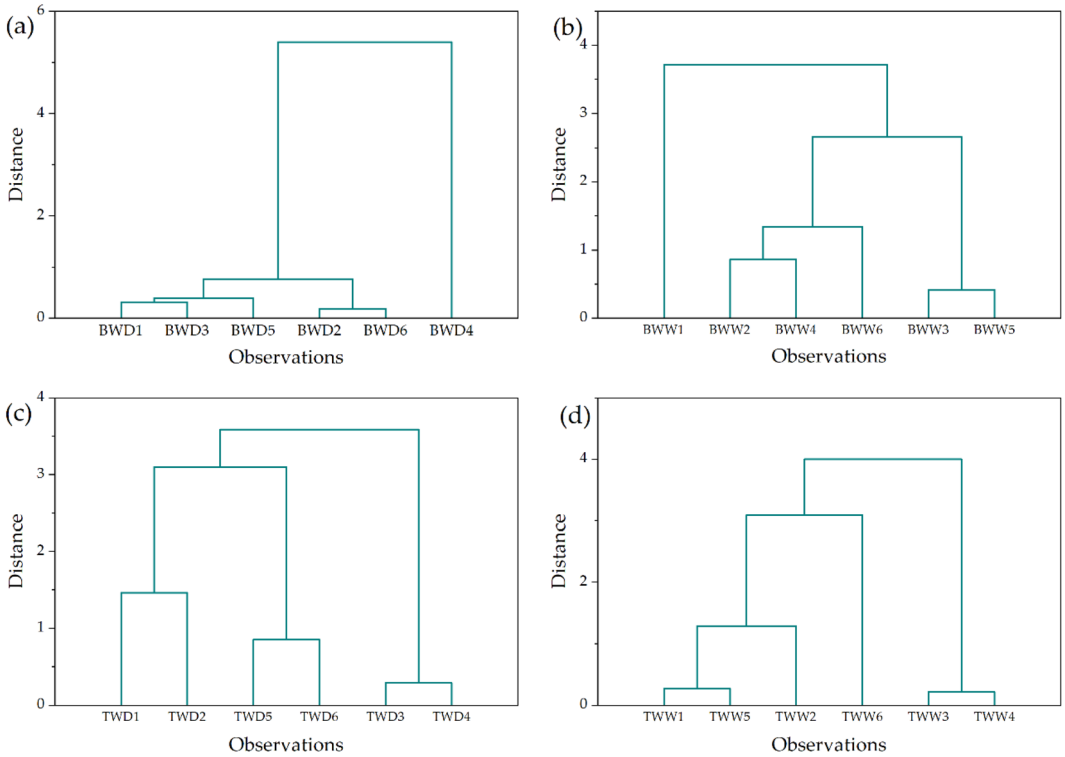

Fig. 13 Dendrogram plot for water samples of (a) Buriganga river in the dry season, (b) Buriganga river in the wet season, (c) Turag river in the dry season, (d) Turag river in the wet season.

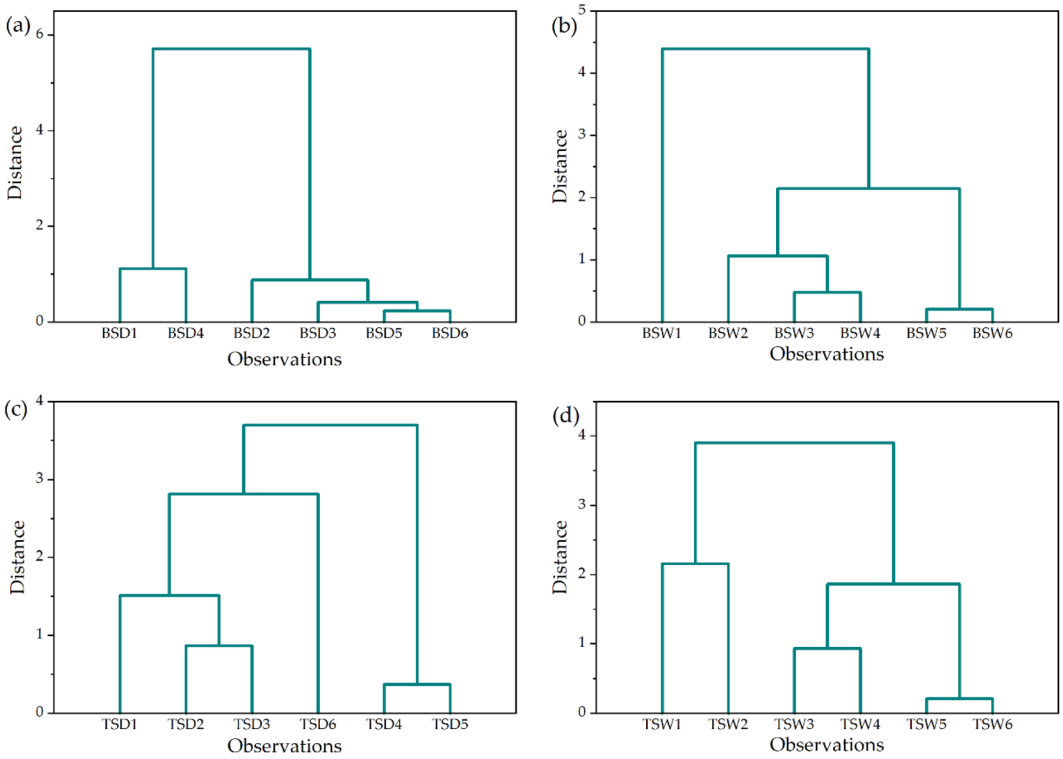

Fig. 14 Dendrogram plot for sediment samples of (a) Buriganga river in the dry season, (b) Buriganga river in the wet season, (c) Turag river in the dry season, (d) Turag river in the wet season.

while water PLI was significantly elevated during dry periods *versus* wet seasons. However, PLI inadequately captures microplastic risk complexity due to the inability to differentiate contaminant composition. Future assessments should integrate polymer-specific risk factors and adsorbed contaminant loads for comprehensive risk characterization.

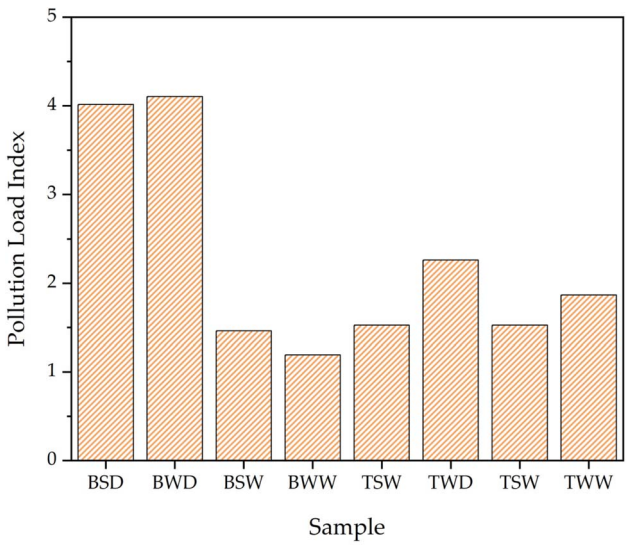

Fig. 15 Pollution load index for the contamination of MPs.

3.8. Comparison of MP abundance with previous studies

Microplastic abundance measurements in the Buriganga and Turag rivers were compared with earlier studies, as detailed in Table 4 (water) and Table 5 (sediment). Haque *et al.* (2023) reported concentrations of 117–250 MPs per L in water (0.1 L samples) and 3500–8170 MPs per kg in sediment (0.003 kg samples) from the Buriganga River.[54] Islam *et al.* (2022) documented lower ranges (4.33 ± 0.58–43.67 ± 0.58 MPs per L water; 17.33 ± 1.53–133.67 ± 5.51 MPs per kg sediment) while detecting multiple polymers (PP, PE, PS, PVC, PET, PA, PES) through $ZnCl_2$ density separation.[67] The present study identified exclusively PE, PP, and PS polymers, attributable to the NaCl separation method, which has reduced efficiency for higher-density polymers. Current Buriganga measurements (dry season: up to 374.84 MPs per L water, 134 330 MPs per kg sediment) exceed earlier values, possibly reflecting methodological differences: larger sample volumes (100 L water/200 g sediment per site) and broader size characterization (>50 μm, despite pore-size limitations) were employed *versus* prior focus on >300 μm particles. Seasonal variation analysis and electrocoagulation removal trials represent additional methodological distinctions. Direct abundance comparisons remain constrained by protocol heterogeneity in sampling volumes, separation techniques, and size detection limits across studies. Reported values should therefore be interpreted as method-influenced estimates rather than absolute environmental baselines.

Table 4 Comparative abundance, sampling, processing, and characterization of MPs in water

Matrices	Sampler	Sampling time	Location	Processing	Characterization	Major types of particles found*	Abundance	Reference
Surface water (100 L)	Plankton net (50 μm)	2023	Buriganga river, Bangladesh	Sieving (50 μm), oven drying (70 °C), WPO, density separation (NaCl), filtration (1.2 μm)	Visual sorting, ATR-FTIR, SEM-EDX	PP, PE, PS	Wet season: 5.17 ± 0.16 to 9.07 ± 0.46 MPs per L Dry season: 26.98 ± 0.15 to 374.84 ± 18.74 MPs per L	This study
Surface water (100 L)	Plankton net (50 μm)	2023	Turag river, Bangladesh	Sieving (50 μm), oven drying (70 °C), WPO, density separation (NaCl), filtration (1.2 μm)	Visual sorting, ATR-FTIR, SEM-EDX	PP, PE, PS	Wet season: 1.93 ± 0.11 to 14.57 ± 0.44 MPs per L Dry season: 3.02 ± 0.19 to 24.76 ± 0.71 MPs per L	This study
Water (0.1 L)	Plastic bottles	Not specified	Buriganga river, Bangladesh	Sieving (2 mm), oven drying (60 °C), digestion (30% H_2O_2), filtration (0.45 μm)	Visual sorting, SEM-EDX, FTIR	PVC, ABS, PET, CA	117–250 MPs/L	54
Surface water (20 L)	Stainless steel mug with a stainless-steel sieve (300 μm)	2021	Buriganga river, Bangladesh	Sieving (300 μm), oven drying (60 °C), digestion (30% H_2O_2), density separation ($ZnCl_2$), filtration (300 μm)	Visual sorting, ATR-FTIR, FE-SEM	PP, PE, PS, PVC, PET, PA, PES	4.33 ± 0.58 to 43.67 ± 0.58 MPs per L	67
Surface water	Manta trawl net	2021	Moheshkhali channel of Bay of Bengal, Bangladesh	WPO; density separation ($ZnCl_2$); sieving (0.63 μm)	Visual sorting, FTIR	PA, PE, PP, PS, PU	0.0001 MPs per L	74
Surface water	Steel bucket	2021	Dhanmondi lake, Gulshan lake, and Hatir Jheel lake, Dhaka, Bangladesh	Digestion (30% H_2O_2), density separation (NaCl), vacuum filtration (20 μm, 0.2 μm), air drying	Visual sorting, ATR-FTIR, SEM	HDPE, LDPE, PVC, PP, PC	36 MPs per L	75
Water	Bulk containers with plankton net (20 μm)	2020	Karnafully river, Bangladesh	Filtration (20 μm)	Visual sorting, μ-FTIR	PE, PET, PP, PA, rayon	0.57 ± 0.07 to 6.63 ± 0.52 MPs per L	76

Table 5 Comparative abundance, sampling, processing, and characterization of MPs in sediment

Matrices	Sampler	Sampling time	Location	Processing	Characterization	Major types of particles found*	Abundance	Reference
Riverbank sediment (200 g)	Stainless steel shovel	2023	Buriganga river, Bangladesh	Sieving (1.2 μm), oven drying (70 °C), digestion (30% H_2O_2), density separation (NaCl), filtration (1.2 μm)	Visual sorting, ATR-FTIR, SEM-EDX	PP, PE, PS	Wet season: 2060 ± 455 to 10 225 ± 1600 MPs per kg Dry season: 11 360 ± 1135 to 134 330 ± 5275 MPs per kg	This study
Riverbank sediment (200 g)	Stainless steel shovel	2023	Turag river, Bangladesh	Sieving (1.2 μm), oven drying (70 °C), digestion (30% H_2O_2), density separation (NaCl), filtration (1.2 μm)	Visual sorting, ATR-FTIR, SEM-EDX	PP, PE, PS	Wet season: 1255 ± 45 to 6590 ± 230 MPs per kg Dry season: 1430 ± 140 to 6720 ± 145 MPs per kg	This study
Riverbed sediment (3 g)	Stainless steel scoop	Not specified	Buriganga river, Bangladesh	Oven drying (60 °C), digestion (30% H_2O_2), density separation (NaCl), centrifugation, filtration (0.45 μm)	Visual sorting, SEM-EDX, FTIR	HDPE, ABS, PET, PS, CA	3500–8170 MPs per kg	54
Sediment (100 g)	Stainless steel scoop	2021	Buriganga river, Bangladesh	Sieving (300 μm), oven drying (60 °C), density separation ($ZnCl_2$), filtration (300 μm)	Visual sorting, ATR-FTIR, FE-SEM	PP, PE, PS, PVC, PET, PA, PES	17.33 ± 1.53 to 133.67 ± 5.51 MPs per kg	67
Riverbank sediment (1 kg)	Stainless steel scoop	2022	Turag river, Bangladesh	Sieving (300 μm), oven drying, WPO, density separation ($ZnCl_2$)	Visual sorting, ATR-FTIR	PP, PE, PS, PC, PET, CA	19.2 ± 2.44 MPs per kg	77
Beach sediment	Stainless-steel ruler and a spoon	2019	Cox's Bazar, Bangladesh	Oven drying (90 °C), sieving (0.3 mm), WPO, density separation ($ZnCl_2$, NaCl), filtration (5 μm)	Visual sorting, ATR-FTIR	PP, PE, PVC, PS, PET, ALK	8.1 ± 2.9 MPs per kg	78
Beach sediment	Metal quadrate	2019	Cox's Bazar, Bangladesh	Oven drying (90 °C), sieving (0.3 mm), WPO, density separation ($ZnCl_2$, NaCl), filtration (5 μm)	Visual sorting	Not specified	200–378.8 MPs per kg (368.68 ± 10.65 MPs per kg)	79
Intertidal sediment	Stainless-steel scrapper	2019	Saint Martin's island, Bangladesh	Oven drying (105 °C), sieving (5, 2.5, 1.25, and 0.625 mm), digestion (30% H_2O_2), density separation (NaCl), filtration (5 μm)	Visual sorting, ATR-FTIR	PA, PE, PU, PS, PP, ALK, époxy, rayon	20–490 MPs per kg	80
Beach sediment	Stainless-steel scrapper	2019	Cox's Bazar, Bangladesh	Sieving (5, 2.5, 1.25, and 0.625 mm)	Visual sorting, ATR-FTIR, SEM	PE, PS, PU, PP, PE-PP	50–1110 MPs per kg	81
Benthic sediment	Ekman grab sampler	2020	Karnafully river, Bangladesh	Oven drying (40 °C), digestion (30% H_2O_2), density separation (NaCl), vacuum filtration (20 μm)	Visual sorting, μ-FTIR	PE, PET, PP, PA, rayon	143.33 ± 3.33 to 1240 ± 5.77 MPs per kg	76

Table 5 (*Contd.*)

Matrices	Sampler	Sampling time	Location	Processing	Characterization	Major types of particles found*	Abundance	Reference
Shore sediment	Stainless steel quadrat	2021	Moheshkhali channel of Bay of Bengal, Bangladesh	WPO; density separation ($ZnCl_2$); filtration (0.45 μm)	Visual sorting, FTIR	PA, PE, PP, PS, PU	6.66–138.33 MPs per m^2	74
Benthic sediment	Eijkelkamp Agrisearch equipment	2021	Dhanmondi Lake, Gulshan Lake, and Hatir Jheel Lake, Dhaka, Bangladesh	Oven drying (65 °C), digestion (30% H_2O_2), density separation (NaCl), filtration	Visual sorting, ATR-FTIR, SEM	HDPE, CA, PC, PP	67 MPs per kg	75

4 Conclusion

Microplastic pollution in urban rivers of Dhaka presents serious ecological and public health threats, especially considering the high population density of this city, inadequate waste management systems, and dependence on these waterways for daily activities. Our research demonstrates substantially greater MP contamination in the Buriganga river compared to the Turag, with sediments serving as primary accumulation zones (dry season maximum: 134 330 MPs per kg sediment). The prevalence of fragments/fibers and PE/PP polymers (75–96%) smaller than 300 μm directly indicates fragmentation of packaging materials and textile industry waste, while MPs carrying heavy metals (Cr, Cd, Pb) confirm their function as pollutant transporters, highlighting the necessity for polymer-specific risk evaluation frameworks. Importantly, electrocoagulation (15 V) proves to be a practical local remediation technique, removing over 99% of MPs within 150 minutes while reducing TDS and TSS levels. These outcomes support environmental protection efforts by focusing interventions on critical areas like Chandir Ghat for specialized cleanup and regulation, confirming the viability of electrocoagulation as an efficient municipal-scale treatment, and guiding policy initiatives for prohibiting single-use plastics near water bodies and enforcing textile waste recycling. Key limitations must be recognized such as the 50 μm net pore size underrepresented smaller particles below 50 μm, resulting in conservative abundance measurements; NaCl density separation favored certain polymers, restricting recovery of higher-density types like PET/PVC and impacting risk evaluations; and electrocoagulation testing on combined particulates leaves polymer-specific removal rates and long-term sludge handling for future investigation. Additionally, multivariate approaches like PCA should be applied in subsequent source analysis to distinguish industrial *versus* municipal inputs. Effective pollution control requires integrated measures, *e.g.*, strict industrial effluent regulations, community-based dry-season monitoring, and technology implementation such as adding electrocoagulation to existing water treatment facilities. Protecting rivers of Dhaka necessitates the immediate application of these approaches with collaborative cross-sector efforts to reduce plastic waste at its source.

Author contributions

Conceptualization: H. R. and M. S. I.; data curation: F. M., H. R., and M. M. K. B.; formal analysis: F. M., and H. R.; funding acquisition: M. S. I; investigation: F. M., and H. R.; methodology: F. M., H. R. and M. S. I; project administration: H. R. and M. S. I; supervision: H. R. and M. S. I.; validation: M. S. I; writing – original draft: F. M.; and H. R., writing – review & editing: F. M., H. R., M. M. K. B. and M. S. I.

Conflicts of interest

The authors declare no potential conflict of interest.

Data availability

The data supporting this article have been included as part of the SI.

Supplementary information: Detailed quantification data of microplastics (MPs) in water and sediment samples from the Buriganga and Turag Rivers, including weight and particle count concentrations. It also includes polymer type identification, elemental composition analysis of MPs, results from electrocoagulation (EC) treatment experiments (including kinetics and a comparison with other studies), pollution load indices, and supporting figures (*e.g.*, FTIR spectra, SEM images, EC setup). available. See DOI: **https://doi.org/10.1039/d5va00118h**.

Acknowledgements

In this work, M. S. I was supported by funds from the Committee for Advanced Studies & Research (CASR), Bangladesh University of Engineering and Technology (BUET), Dhaka-1000, Bangladesh. In addition, H. R. and M. S. I. acknowledge the technical support received from the Water Resources Planning Organization (WARPO), Bangladesh, and laboratory support from the Department of Chemical Engineering, BUET.

References

1 S. Braun Why most plastic can't be recycled – DW – 03/17/2023. dw.com 2023; available from: **https://www.dw.com/en/why-most-plastic-cant-be-recycled/a-64978847**.
2 G. Z. Dodson, *et al.*, Microplastic fragment and fiber contamination of beach sediments from selected sites in Virginia and North Carolina, USA, *Mar. Pollut. Bull.*, 2020, **151**, 110869.
3 M. Fardullah, *et al.*, Occurrence and spatial distribution of microplastics in water and sediments of Hatiya Island, Bangladesh and their risk assessment, *J. Environ. Manage.*, 2024, **370**, 122697.
4 Y. Picó and D. Barceló, Analysis and Prevention of Microplastics Pollution in Water: Current Perspectives and Future Directions, *ACS Omega*, 2019, **4**(4), 6709–6719.
5 R. Qi, *et al.*, Behavior of microplastics and plastic film residues in the soil environment: A critical review, *Sci. Total Environ.*, 2020, **703**, 134722.
6 R. Saborowski, E. Paulischkis and L. Gutow, How to get rid of ingested microplastic fibers? A straightforward approach of the Atlantic ditch shrimp Palaemon varians, *Environ. Pollut.*, 2019, **254**, 113068.
7 S. Taheri, *et al.*, Investigating the pollution of bottled water by the microplastics (MPs): the effects of mechanical stress, sunlight exposure, and freezing on MPs release, *Environ. Monit. Assess.*, 2022, **195**(1), 62.
8 UNEP. Visual Feature | Beat Plastic Pollution, available from: **https://www.unep.org/interactives/beat-plastic-pollution/?gclid=CjwKCAjwwb6lBhBJEiwAbuVUShn9_A9u08RRVxC8qVDNt0naNYymJtQUZMbGkH0CO2YfHLveLuhFXBoC1LIQAvD_BwE**.
9 T. Islam, *et al.*, Microplastic pollution in Bangladesh: Research and management needs, *Environ. Pollut.*, 2022, **308**, 119697.
10 S. Yoshijima, *et al.*, *Towards a Multisectoral Action Plan for Sustainable Plastic Management in Bangladesh*, World Bank, 2021.
11 G. Lamichhane, *et al.*, Microplastics in environment: global concern, challenges, and controlling measures, *Int. J. Environ. Sci. Technol.*, 2022, **20**(4), 4673–4694.
12 L. An, *et al.*, Sources of Microplastic in the Environment, in *Microplastics in Terrestrial Environments: Emerging Contaminants and Major Challenges*, ed. D. He and Y. Luo, Springer International Publishing, Cham, 2020, pp. 143–159.
13 T. S. M. Amelia, *et al.*, Marine microplastics as vectors of major ocean pollutants and its hazards to the marine ecosystem and humans, *Prog. Earth Planet. Sci.*, 2021, **8**(1), 12.
14 C. Zhang, *et al.*, Toxic effects of microplastic on marine microalgae Skeletonema costatum: Interactions between microplastic and algae, *Environ. Pollut.*, 2017, **220**, 1282–1288.
15 J. S. Choi, *et al.*, Toxicological effects of irregularly shaped and spherical microplastics in a marine teleost, the sheepshead minnow (Cyprinodon variegatus), *Mar. Pollut. Bull.*, 2018, **129**(1), 231–240.
16 Y. Meng, F. J. Kelly and S. L. Wright, Advances and challenges of microplastic pollution in freshwater ecosystems: A UK perspective, *Environ. Pollut.*, 2020, **256**, 113445.
17 S. Sarijan, *et al.*, Microplastics in freshwater ecosystems: a recent review of occurrence, analysis, potential impacts, and research needs, *Environ. Sci. Pollut. Res.*, 2021, **28**(2), 1341–1356.
18 K. Blackburn and D. Green, The potential effects of microplastics on human health: What is known and what is unknown, *Ambio*, 2022, **51**(3), 518–530.
19 Y. Li, *et al.*, Potential Health Impact of Microplastics: A Review of Environmental Distribution, Human Exposure, and Toxic Effects, *Environ. Health*, 2023, **1**(4), 249–257.
20 S. Mhiret Gela and T. A. Aragaw, Abundance and Characterization of Microplastics in Main Urban Ditches Across the Bahir Dar City, Ethiopia, *Front. Environ. Sci.*, 2022, **10**, 831417.
21 S. Usman, *et al.*, The Burden of Microplastics Pollution and Contending Policies and Regulations, *Int. J. Environ. Res. Public Health*, 2022, **19**(11), 6773.
22 A. Ashrafy, *et al.*, Microplastics Pollution: A Brief Review of Its Source and Abundance in Different Aquatic Ecosystems, *J. Hazard. Mater. Adv.*, 2023, **9**, 100215.
23 M. Gholizadeh, *et al.*, Abundance and characteristics of microplastic in some commercial species from the Persian Gulf, Iran, *J. Environ. Manage.*, 2023, **344**, 118386.
24 Y. Xu, *et al.*, Microplastic pollution in Chinese urban rivers: The influence of urban factors, *Resour., Conserv. Recycl.*, 2021, **173**, 105686.

25 T. Bashar and I. W. Fung, Water Pollution in a Densely Populated Megapolis, Dhaka, *Water*, 2020, **12**(8), 2124.
26 M. N. Hossain, *et al.*, Comparative seasonal assessment of pollution and health risks associated with heavy metals in water, sediment and Fish of Buriganga and Turag River in Dhaka City, Bangladesh, *SN Appl. Sci.*, 2021, **3**(4), 509.
27 M. R. Islam and M. G. Mostafa, Textile Dyeing Effluents and Environment Concerns - A Review, *J. Environ. Sci. Nat. Resour.*, 2019, **11**(1–2), 131–144.
28 F. Mahmud, *et al.*, Antibiotic-contaminated wastewater treatment and remediation by electrochemical advanced oxidation processes (EAOPs), *Groundw. Sustain. Dev.*, 2024, **25**, 101181.
29 B. Nath Roy, *et al.*, Principal component analysis incorporated water quality index modeling for Dhaka-based rivers, *City Environ. Interact.*, 2024, **23**, 100150.
30 M. Pivokonsky, *et al.*, Occurrence of microplastics in raw and treated drinking water, *Sci. Total Environ.*, 2018, **643**, 1644–1651.
31 M. Pivokonský, *et al.*, Occurrence and fate of microplastics at two different drinking water treatment plants within a river catchment, *Sci. Total Environ.*, 2020, **741**, 140236.
32 T. K. Dey, M. E. Uddin and M. Jamal, Detection and removal of microplastics in wastewater: evolution and impact, *Environ. Sci. Pollut. Res.*, 2021, **28**(14), 16925–16947.
33 D. Elkhatib, V. Oyanedel-Craver and E. Carissimi, Electrocoagulation applied for the removal of microplastics from wastewater treatment facilities, *Sep. Purif. Technol.*, 2021, **276**, 118877.
34 R. Y. Krishnan, *et al.*, Recent approaches and advanced wastewater treatment technologies for mitigating emerging microplastics contamination – A critical review, *Sci. Total Environ.*, 2023, **858**, 159681.
35 Y. Jeong, *et al.*, Transformation of microplastics by oxidative water and wastewater treatment processes: A critical review, *J. Hazard. Mater.*, 2023, **443**, 130313.
36 A. Mahmud, *et al.*, Aquatic Microplastic Pollution Control Strategies: Sustainable Degradation Techniques, Resource Recovery, and Recommendations for Bangladesh, *Water*, 2022, **14**(23), 3968.
37 Y. Pan, *et al.*, Removing microplastics from aquatic environments: A critical review, *Environ. Sci. Ecotechnology*, 2023, **13**, 100222.
38 C. Akarsu, H. Kumbur and A. E. Kideys, Removal of microplastics from wastewater through electrocoagulation-electroflotation and membrane filtration processes, *Water Sci. Technol.*, 2021, **84**(7), 1648–1662.
39 S. Akter and M. S. Islam, Effect of additional Fe2+ salt on electrocoagulation process for the degradation of methyl orange dye: An optimization and kinetic study, *Heliyon*, 2022, **8**(8), e10176.
40 S. Akter, M. B. K. Suhan and M. S. Islam, Recent advances and perspective of electrocoagulation in the treatment of wastewater: A review, *Environ. Nanotechnol., Monit. Manage.*, 2022, **17**, 100643.
41 S. Sadaf, *et al.*, Electrocoagulation-based wastewater treatment process and significance of anode materials for the overall improvement of the process: A critical review, *Water Process Eng.*, 2024, **62**, 105409.
42 M. B. K. Suhan, *et al.*, Comparative degradation study of remazol black B dye using electro-coagulation and electro-Fenton process: Kinetics and cost analysis, *Environ. Nanotechnol., Monit. Manage.*, 2020, **14**, 100335.
43 P. S. Kumar, Chapter eight - Microplastics and its removal strategies from marine water, in *Modern Treatment Strategies for Marine Pollution*, ed. P. S. Kumar, Elsevier, 2021, pp. 125–144.
44 W. Perren, A. Wojtasik and Q. Cai, Removal of Microbeads from Wastewater Using Electrocoagulation, *ACS Omega*, 2018, **3**(3), 3357–3364.
45 M. Luo, *et al.*, Removal and toxic forecast of microplastics treated by electrocoagulation: Influence of dissolved organic matter, *Chemosphere*, 2022, **308**, 136309.
46 M. Shen, *et al.*, Efficient removal of microplastics from wastewater by an electrocoagulation process, *Chem. Eng. J.*, 2022, **428**, 131161.
47 R. Xu, *et al.*, Removal of microplastics and attached heavy metals from secondary effluent of wastewater treatment plant using interpenetrating bipolar plate electrocoagulation, *Sep. Purif. Technol.*, 2022, **290**, 120905.
48 S. Cunsolo, *et al.*, Optimising sample preparation for FTIR-based microplastic analysis in wastewater and sludge samples: multiple digestions, *Anal. Bioanal. Chem.*, 2021, **413**(14), 3789–3799.
49 D. L. Tomlinson, *et al.*, Problems in the assessment of heavy-metal levels in estuaries and the formation of a pollution index, *Helgol. Mar. Res.*, 1980, **33**(1), 566–575.
50 P. Xu, *et al.*, Microplastic risk assessment in surface waters: A case study in the Changjiang Estuary, China, *Mar. Pollut. Bull.*, 2018, **133**, 647–654.
51 E. Arena, *et al.*, Effects of Light Exposure, Bottle Colour and Storage Temperature on the Quality of Malvasia delle Lipari Sweet Wine, *Foods*, 2021, **10**(8), 1881.
52 B. Smith, The Infrared Spectra of Polymers II: Polyethylene, *Spectroscopy*, 2021, **36**(9), 24–29.
53 D. Deswati, *et al.*, Preliminary detection of microplastics in surface water of Maninjau Lake in Agam, Indonesia, *AACL Bioflux*, 2023, **16**, 2601–2614.
54 M. R. Haque, *et al.*, Assessment of microplastics pollution in aquatic species (fish, crab, and snail), water, and sediment from the Buriganga River, Bangladesh: An ecological risk appraisals, *Sci. Total Environ.*, 2023, **857**, 159344.
55 J. Frias, *et al.*, Standardised protocol for monitoring microplastics in sediments. JPI-Oceans BASEMAN project, 2018, DOI: **10.13140/RG.2.2.36256.89601/1**.
56 H. K. Imhof, *et al.*, A novel, highly efficient method for the separation and quantification of plastic particles in sediments of aquatic environments: Novel plastic particle separation method, *Limnol. Oceanogr.:Methods*, 2012, **10**(7), 524–537.
57 Institute for E. Sustainability and M.T.S.o.M. Litter, *Guidance on Monitoring of Marine Litter in European Seas*, Publications Office of the European Union, LU, 2013.

58 M. Firdaus, Y. Trihadiningrum and P. Lestari, Microplastic pollution in the sediment of Jagir Estuary, Surabaya City, Indonesia, *Mar. Pollut. Bull.*, 2020, **150**, 110790.
59 B. Smith, Library Searching, *Spectroscopy*, 2021, **36**(3), 24–27.
60 B. Smith, Infrared Spectroscopy of Polymers, VIII: Polyesters and the Rule of Three, *Spectroscopy*, 2022, **37**(10), 25–28.
61 B. Smith, Infrared Spectroscopy of Polymers, XI: Introduction to Organic Nitrogen Polymers, *Spectroscopy*, 2023, **38**(03), 14–18.
62 S. Prajapati, *et al.*, Qualitative and quantitative analysis of microplastics and microfiber contamination in effluents of the City of Saskatoon wastewater treatment plant, *Environ. Sci. Pollut. Res.*, 2021, **28**(25), 32545–32553.
63 T. Tsering, *et al.*, Microplastics pollution in the Brahmaputra River and the Indus River of the Indian Himalaya, *Sci. Total Environ.*, 2021, **789**, 147968.
64 N. M. Ainali, D. N. Bikiaris and D. A. Lambropoulou, Aging effects on low- and high-density polyethylene, polypropylene and polystyrene under UV irradiation: An insight into decomposition mechanism by Py-GC/MS for microplastic analysis, *J. Anal. Appl. Pyrolysis*, 2021, **158**, 105207.
65 K. Miserli, *et al.*, Screening of Microplastics in Aquaculture Systems (Fish, Mussel, and Water Samples) by FTIR, Scanning Electron Microscopy–Energy Dispersive Spectroscopy and Micro-Raman Spectroscopies, *Applied Sciences*, 2023, **13**(17), 9705.
66 N. Oveisy, *et al.*, Occurrence, identification, and discharge of microplastics from effluent and sludge of the largest WWTP in Iran—South of Tehran, *Water Environ. Res.*, 2022, **94**(8), e10765.
67 M. S. Islam, Z. Islam and M. R. Hasan, Pervasiveness and characteristics of microplastics in surface water and sediment of the Buriganga River, Bangladesh, *Chemosphere*, 2022, **307**, 135945.
68 Y. Cao, *et al.*, A critical review on the interactions of microplastics with heavy metals: Mechanism and their combined effect on organisms and humans, *Sci. Total Environ.*, 2021, **788**, 147620.
69 J. Patterson, *et al.*, Microplastic and heavy metal distributions in an Indian coral reef ecosystem, *Sci. Total Environ.*, 2020, **744**, 140706.
70 S. Liu, *et al.*, Microplastics as a vehicle of heavy metals in aquatic environments: A review of adsorption factors, mechanisms, and biological effects, *J. Environ. Manage.*, 2022, **302**, 113995.
71 N. Majed, *et al.*, How dynamic is the heavy metals pollution in the Buriganga River of Bangladesh? A spatiotemporal assessment based on environmental indices, *Int. J. Environ. Sci. Technol.*, 2022, **19**(5), 4181–4200.
72 S. Mitra, *et al.*, Impact of heavy metals on the environment and human health: Novel therapeutic insights to counter the toxicity, *J. King Saud Univ., Sci.*, 2022, **34**(3), 101865.
73 G. Wang, *et al.*, Seasonal variation and risk assessment of microplastics in surface water of the Manas River Basin, China, *Ecotoxicol. Environ. Saf.*, 2021, **208**, 111477.
74 S. Al Nahian, *et al.*, Distribution, characteristics, and risk assessments analysis of microplastics in shore sediments and surface water of Moheshkhali channel of Bay of Bengal, Bangladesh, *Sci. Total Environ.*, 2023, **855**, 158892.
75 F. T. Mercy, A. K. M. R. Alam and M. A. Akbor, Abundance and characteristics of microplastics in major urban lakes of Dhaka, Bangladesh, *Heliyon*, 2023, **9**(4), e14587.
76 M. J. Hossain, *et al.*, Surface water, sediment, and biota: The first multi-compartment analysis of microplastics in the Karnafully river, Bangladesh, *Mar. Pollut. Bull.*, 2022, **180**, 113820.
77 M. B. Khan, *et al.*, Abundance, distribution and composition of microplastics in sediment and fish species from an Urban River of Bangladesh, *Sci. Total Environ.*, 2023, **885**, 163876.
78 S. M. A. Rahman, *et al.*, Occurrence and spatial distribution of microplastics in beach sediments of Cox's Bazar, Bangladesh, *Mar. Pollut. Bull.*, 2020, **160**, 111587.
79 M. B. Hossain, *et al.*, Abundance and characteristics of microplastics in sediments from the world's longest natural beach, Cox's Bazar, Bangladesh, *Mar. Pollut. Bull.*, 2021, **163**, 111956.
80 M. Tajwar, *et al.*, Microplastic contamination in the sediments of the Saint Martin's Island, Bangladesh, *Reg. Stud. Mar. Sci*, 2022, **53**, 102401.
81 M. Tajwar, M. Yousuf Gazi and S. K. Saha, Characterization and Spatial Abundance of Microplastics in the Coastal Regions of Cox's Bazar, Bangladesh: An Integration of Field, Laboratory, and GIS Techniques, *Soil Sediment Contam.: Int. J.*, 2022, **31**(1), 57–80.